Government of **Western Australia**
Department of **Mines and Petroleum**

RECORD 2013/5

PETROGENESIS OF GABBROS OF THE MESOPROTEROZOIC FRASER ZONE: CONSTRAINTS ON THE TECTONIC EVOLUTION OF THE ALBANY–FRASER OROGEN

by
RH Smithies, CV Spaggiari, CL Kirkland, HM Howard and WD Maier



Geological Survey of Western Australia

Government of **Western Australia**
Department of **Mines and Petroleum**

Record 2013/5

PETROGENESIS OF GABBROS OF THE MESOPROTEROZOIC FRASER ZONE: CONSTRAINTS ON THE TECTONIC EVOLUTION OF THE ALBANY–FRASER OROGEN

by
RH Smithies, CV Spaggiari, CL Kirkland, HM Howard, and WD Maier[1]

[1] **Department of Geosciences, University of Oulu, Linnanmaa, Oulu 90014, Finland**

Perth 2013

Geological Survey of Western Australia

REFERENCE
The recommended reference for this publication is:
Smithies, RH, Spaggiari, CV, Kirkland, CL, Howard, HM and Maier, WD 2011, Petrogenesis of gabbros of the Mesoproterozoic Fraser Zone: constraints on the tectonic evolution of the Albany–Fraser Orogen: Geological Survey of Western Australia, Record 2013/5, 29p.

National Library of Australia Card Number and ISBN 978-1-74168-480-3

Grid references in this publication refer to the Geocentric Datum of Australia 1994 (GDA94). Locations mentioned in the text are referenced using Map Grid Australia (MGA) coordinates, Zone 51. All locations are quoted to at least the nearest 100 m.

Published 2013 by Geological Survey of Western Australia
This Record is published in digital format (PDF) and is available online at <http://www.dmp.wa.gov.au/GSWApublications>.

Further details of geological products and maps produced by the Geological Survey of Western Australia are available from:
Information Centre
Department of Mines and Petroleum
100 Plain Street
EAST PERTH WESTERN AUSTRALIA 6004
Telephone: +61 8 9222 3459 Facsimile: +61 8 9222 3444
www.dmp.wa.gov.au/GSWApublications

Contents

Figures

Appendices

Petrogenesis of gabbros of the Mesoproterozoic Fraser Zone: constraints on the tectonic evolution of the Albany–Fraser Orogen

by

RH Smithies, CV Spaggiari, CL Kirkland, HM Howard, and WD Maier[1]

Abstract

Forty-five samples of metagabbro sheets from the c. 1300 Ma Fraser Zone of the Albany–Fraser Orogen have been analysed for major and trace element geochemistry. The geochemical range corresponds with previously published ranges for metagabbros from this region. Two broad groups can be recognized: the 'main gabbros' which show no field, petrographic, or geochemical evidence of having interacted with country-rock, and the 'hybrid gabbros' which show considerable evidence for such interaction. The hybrid gabbros can be further subdivided geochemically into low La/Th rocks that have incorporated material from contemporaneous high-Th monzogranitic sheets (Group 1 hybrid gabbros), and high La/Th rocks that have assimilated low-degree partial melts of metasedimentary country rock at the level of emplacement (Group 2 hybrid gabbros). The main gabbros are parental to the hybrid gabbros but escaped hybridization during ascent or emplacement. However, they still contain an enriched crustal component acquired at a deeper level. Previous accounts have suggested this enrichment reflects a subduction addition to the mantle sources that formed a series of discrete, subsequently accreted, ocean island arcs. All previous and recent Nd- and Hf-isotopic data are inconsistent with that interpretation and trace element enrichments are better explained in terms of assimilation of basement that included a Sr-depleted component of Archean, or reworked Archean, crust. Following early basement contamination, the main gabbro sheets that comprise the dominant component of the Fraser Zone were emplaced into a lower crustal hot-zone where they variably mixed with contemporaneous granite magma and country-rock melts. The presence of voluminous gabbroic sheets, regional granite magmatism, and previously published peak metamorphic conditions of >800°C and >8 kbars in metasedimentary rocks are all indicative of a regional thermal anomaly from at least 1305 to 1290 Ma that coincided with the formation of the Fraser Zone. Based on these findings, and on a range of other recent geological evidence, the preferred tectonic setting is either a distal back-arc or an intercontinental rift.

KEYWORDS: Mesoproterozoic; gabbro; geochemistry; Fraser Zone; tectonic setting; Albany–Fraser Orogen.

Introduction

The Albany–Fraser Orogen lies along the southern and southeastern margins of the Archean Yilgarn Craton, and is part of the West Australian Craton (Fig. 1). The orogen is dominated by Paleoproterozoic and Mesoproterozoic rocks, the formation of which involved the reworking of the southern Yilgarn Craton from at least 1800 Ma through to 1140 Ma (Spaggiari et al., 2011). The Fraser Zone is one of several northeast-trending tectonic subdivisions of the orogen (Fig. 1; Spaggiari et al., 2009), and is dominated by metagabbroic rocks that have previously been interpreted as representing the remnants of one or more c. 1300 Ma oceanic arcs that accreted onto the Yilgarn Craton during closure of an ocean separating the Yilgarn and Mawson Cratons (Condie and Myers, 1999). This interpretation had a significant influence on subsequent models for the Mesoproterozoic tectonic evolution of southwestern and central Australia (Clark et al., 2000; Bodorkos and Clark, 2004a).

The Northern Foreland of the Albany–Fraser Orogen comprises reworked Archean rocks of the Yilgarn Craton (Fig. 1; Spaggiari et al., 2009). Additionally, fragments of Archean crust, interpreted to be remnants of the Yilgarn Craton, are preserved within the Paleoproterozoic crust of the orogen (Kirkland et al., 2011a; Spaggiari et al., 2011). Recent geochronological and isotopic studies, summarized in Spaggiari et al. (2011), have found that both Archean and Paleoproterozoic crust extends significantly farther to the south and east than previously assumed. The presence of Archean basement in these regions is implied by the outcropping Archean fragments, and also by nonradiogenic source components in Proterozoic granites. Thus, the accumulating evidence that Archean basement components underlie much of the Albany–Fraser Orogen, possibly including the Fraser Zone, significantly challenges the accreted oceanic-arc hypothesis for the Fraser Zone. Indeed, a recent reinterpretation of the

[1] Department of Geosciences, University of Oulu, Linnanmaa, Oulu 90014, Finland

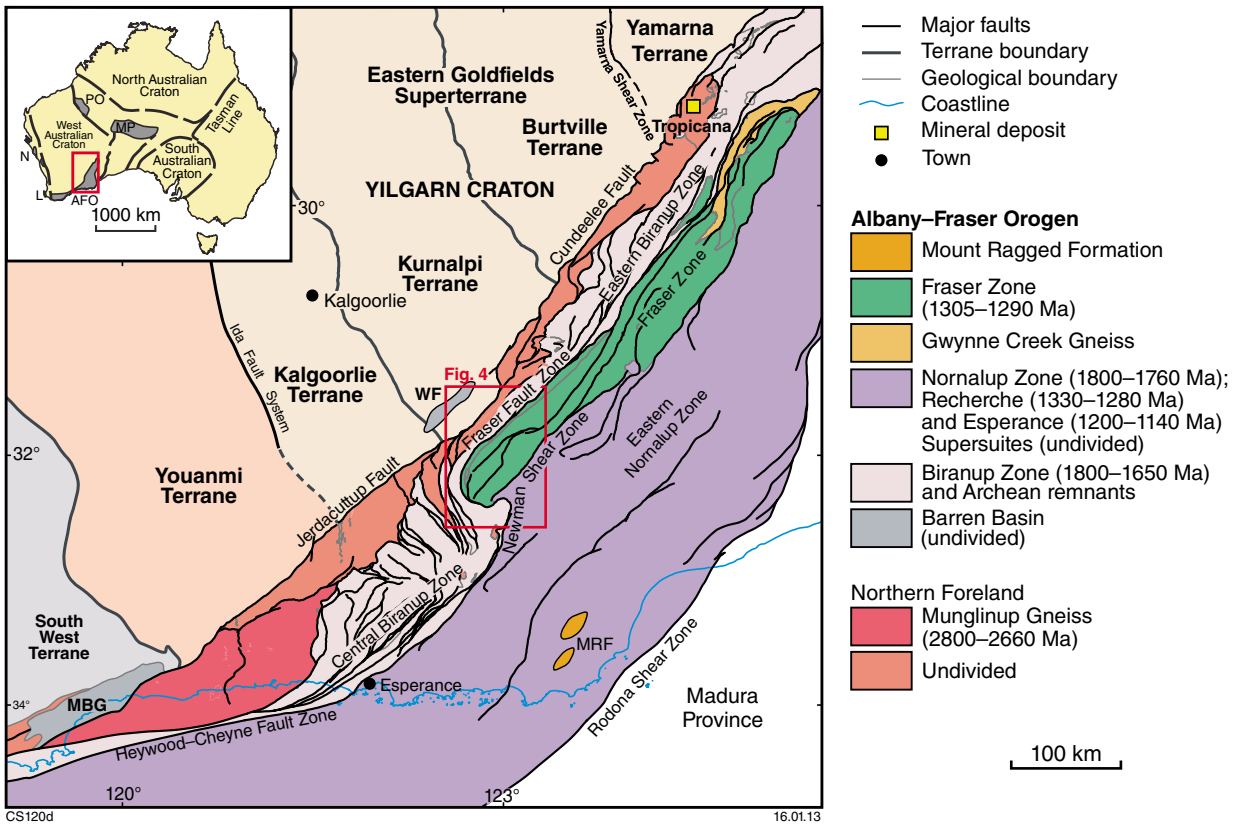

Figure 1. **Simplified, pre-Mesozoic interpreted bedrock geology of the east Albany–Fraser Orogen and tectonic subdivisions of the Yilgarn Craton (modified from Spaggiari et al., 2009; Geological Survey of Western Australia, 2011; Cassidy et al., 2006; Pawley et al., 2012). Abbreviations used: MBG – Mount Barren Group; WF – Woodline Formation; MRF – Mount Ragged Formation; AFO – Albany–Fraser Orogen; MP – Musgrave Province; PO – Paterson Orogen; L – Leeuwin Province; N – Northhampton Province.**

tectonic setting for the Fraser Zone suggested formation within either a back-arc or rift setting (Spaggiari et al., 2011), in what could be considered as a Mesoproterozoic geodynamic repetition of similar events that occurred on the same margin during the late Paleoproterozoic (Kirkland et al., 2011a).

The accreted oceanic-arc hypothesis for the Fraser Zone was based on geochemical similarities between the Fraser Zone gabbros and mafic rocks formed in modern subduction zones (Condie and Myers, 1999). This Record presents new geochemical results from the metamorphosed gabbros of the Fraser Zone, with the aim of critically re-evaluating the geochemical evidence for trace element enrichments indicating a subduction-modified mantle source for the Fraser Zone gabbros.

Regional setting

The Albany–Fraser Orogen is truncated to the west by the late Meso- to Neoproterozoic Darling Fault Zone and Pinjarra Orogen. Its northeastern and eastern extents are covered by the Neoproterozoic to Paleozoic Officer and Gunbarrel Basins, and by the Cretaceous to Cenozoic Eucla Basin. The orogen is divided into two main tectonic components that reflect its relationship to the Yilgarn Craton: the Archean Northern Foreland, and the predominantly younger, Paleo- to Mesoproterozoic Kepa Kurl Booya Province (Spaggiari et al., 2009). The Northern Foreland is the portion of the Archean Yilgarn Craton that was reworked during the Albany–Fraser Orogeny. It consists of greenschist and amphibolite to granulite facies Archean gneisses and granites, remnant greenstones, and younger dolerite dykes (Myers, 1990; Spaggiari et al., 2009). In the northeastern part of the orogen, the Northern Foreland is intruded by Paleoproterozoic granites of the Biranup Zone (Spaggiari et al., 2011; Spaggiari and Pawley, 2012a). The Munglinup Gneiss, a major component of the Northern Foreland preserved in thrust sheets in the central part of the orogen, was interpreted by Myers et al. (1996) as an allochthonous Archean unit thrust over the Yilgarn Craton. However, more recent geochronology from the Munglinup Gneiss clearly indicates that it represents overprinted Archean Yilgarn Craton rocks with protolith ages of 2717–2640 Ma (e.g. GSWA 83691, Nelson, 1995). Hafnium isotopes in magmatic zircon grains from the Northern Foreland yield model ages clustering at c. 3.2 Ga, which implies a reworked Archean Hf source, similar in crustal residence time to many intrusive rocks within the Eastern Goldfields Superterrane (Kirkland et al., 2011b).

The Kepa Kurl Booya Province has been defined as the various Proterozoic crustal components affected by, and probably amalgamated by, 1345–1260 Ma Stage I tectonism during the Albany–Fraser Orogeny (Spaggiari et al., 2009). It includes three, geographical and structural, fault-bounded zones defined as the Biranup, Fraser, and Nornalup Zones (Fig. 1; Spaggiari et al., 2009).

The Biranup Zone lies along the entire southern and southeastern margin of the Yilgarn Craton, adjacent to and interleaved with the Northern Foreland (Fig. 1). It is dominated by intensely deformed, amphibolite- to granulite-facies orthogneiss, metagabbro, and paragneiss, with ages of c. 1800–1625 Ma (Nelson et al., 1995; Spaggiari et al., 2009, 2011). The lack of geochronological evidence for a Paleoproterozoic magmatic or tectonothermal event in the southern Yilgarn Craton during this period led to the suggestion that the Biranup Zone was an exotic terrane accreted to the Yilgarn Craton margin during Stage I of the Albany–Fraser Orogeny (e.g. Nelson et al., 1995; Clark et al., 2000; Spaggiari et al., 2009). However, the discovery of fragments of Archean metagranite within the Biranup Zone, which have typical Yilgarn Craton granite ages, and Lu–Hf data from Biranup Zone granitic rocks, have clearly shown that the Biranup Zone is autochthonous, and was formed by modification of Yilgarn Craton crust (Kirkland et al., 2011a, 2011b; Spaggiari et al., 2011).

The Nornalup Zone is the southern- and eastern-most known unit of the Albany–Fraser Orogen (Fig. 1; Myers, 1990, 1995). In the east, the Nornalup Zone is separated from the Biranup and Fraser Zones by the Newman Shear Zone and Boonderoo Fault, and from the Madura Province by the Rodona Shear Zone (Spaggiari et al., 2012). Recently dated metamorphic rocks from the Nornalup Zone include migmatitic monzogranitic gneiss containing angular mafic inclusions that yield a date of 1809 ± 8 Ma, interpreted as the age of magmatic crystallization of the monzogranite (GSWA 194785, preliminary data). This, and the presence of 1763 ± 11 Ma granitic gneiss (GSWA 194784, preliminary data) from the Newman Shear Zone, indicate that the Nornalup Zone contains Paleoproterozoic granitic rocks, similar in age to those in the Biranup Zone. The southeastern part of the Biranup Zone, and most of the Nornalup Zone, contain voluminous intrusions of granitic rocks of the 1330–1280 Ma Recherche Supersuite and the 1200–1140 Ma Esperance Supersuite (Myers, 1995; Nelson et al., 1995; Spaggiari et al., 2011; Spaggiari and Pawley, 2012b).

Supracrustal rocks of the Albany–Fraser Orogen occur in three major basins that reflect three cycles of sedimentation and basin formation: the Paleoproterozoic Barren Basin, and the Mesoproterozoic Arid and Ragged Basins (Spaggiari et al., 2011). The Barren Basin includes the c. 1800 Ma Stirling Range Formation, the c. 1700 Ma Mount Barren Group and Woodline Formation, the c. 1620 Ma Fly Dam Formation, and several unnamed occurrences of metasedimentary rocks (Dawson et al., 2003; Rasmussen et al., 2004; Vallini et al., 2005; Hall et al., 2008; Spaggiari et al., 2011). These successions represent the first major cycle of sedimentation in the Albany–Fraser Orogen, with ongoing sedimentation concurrent with the 1710–1650 Ma Biranup Orogeny. The Arid Basin represents the second major cycle of sedimentation, deposited prior to and during the early part of Stage I of the Albany–Fraser Orogeny, up to at least 1330 Ma (Spaggiari et al., 2011). It includes metasedimentary rocks of the Fraser Range Metamorphics, the Gwynne Creek Gneiss, and the Malcolm Metamorphics (previously Malcolm Gneiss of Myers, 1995; Nelson et al., 1995; Clark et al., 1999; Spaggiari et al., 2011; Adams, 2012). The Ragged Basin is a more restricted succession representing the third cycle of sedimentation in the orogen, and includes the Mount Ragged Formation and the Salisbury Gneiss, which are interpreted to have been deposited after c. 1260 Ma, following Stage I of the Albany–Fraser Orogeny (Clark et al., 2000).

Fraser Zone

The Fraser Zone is dominated by high-grade rocks that have a strong, distinct geophysical signature in both aeromagnetic and gravity data — the latter reflecting high density attributed to the dominance of metagabbroic rocks (Fig. 2). The northern part of the Fraser Zone is covered by younger rocks of the Eucla Basin, but the gravity data indicate that it is an approximately 425 km long, northeasterly trending, fault-bounded unit that is up to 50 km wide (Spaggiari and Pawley, 2012b). The zone contains the Fraser Range Metamorphics (Spaggiari et al., 2009), which are dominated by metagabbroic rocks with sheets of metagranitic material and layers of pelitic, semipelitic to calcic, and locally iron-rich metasedimentary rocks (Clark, 1999; Oorschot, 2011; Spaggiari et al., 2011). Peak metamorphic temperatures and pressures recorded in the metasedimentary rocks reached 800–850°C and 8–9 kbar (Clark, 1999; Oorschot, 2011). The pressure estimates indicate depths of 25–30 km, which may constrain the depth at which the presently exposed gabbros were intruded, and also the minimum depth of the basin into which the siliciclastic rocks accumulated. However, the peak metamorphic assemblages that define the P–T estimates grew in early, gneissic, deformation-related fabrics that are presently unconstrained with respect to particular structures (Clark, 1999; Oorschot, 2011). The P–T conditions could therefore also relate to burial by crustal thickening, or alternatively, could relate to extensional fabrics that formed during intrusion of the magmatic rocks.

The limited available geochemical data for felsic rocks within the Fraser Zone <http://geochem.dmp.wa.gov.au/geochem/> permits these rocks to be subdivided into two broad groups: one compositionally similar to granites representing the majority of the 1330–1280 Ma Recherche Supersuite, the other likely reflecting magmas derived locally through melting of the metasedimentary components of the Fraser Zone (see below).

The metagabbros of the Fraser Zone occur as thin to voluminous sheets that range in thickness from several centimetres up to several hundred metres. Where these rocks outcrop in the southern portion of the Fraser Zone, the gabbroic sheets appear to thicken from the northwest

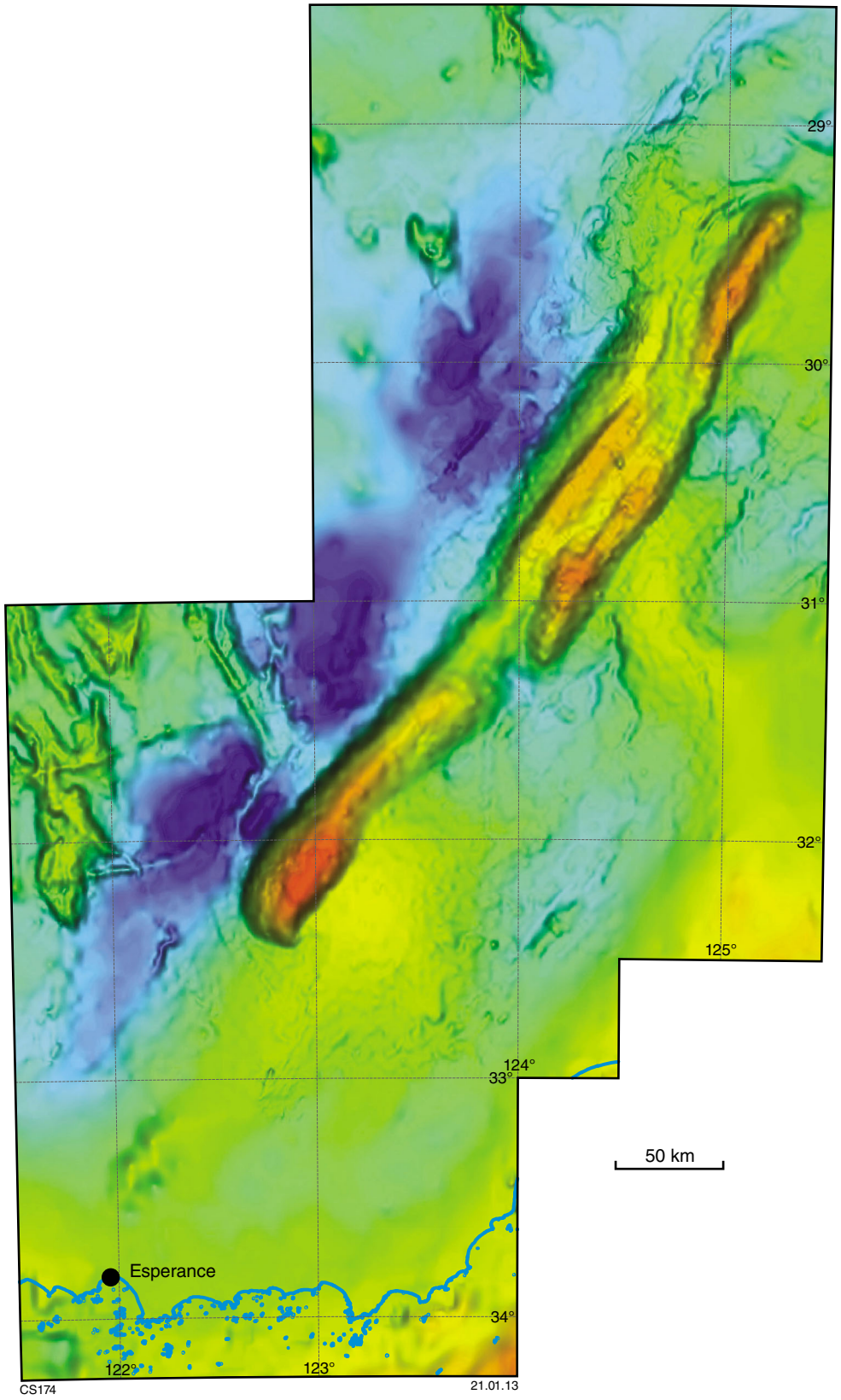

Figure 2. Gravity image showing full extent of the Fraser Zone (from Spaggiari and Pawley, 2012c).

— where they mainly intrude metasedimentary rocks as thin sills mostly concordant with bedding — to the southeast, where they are volumetrically dominant. Sheets of granitic material ranging from cm-scale to 10s of metres thickness are interlayered with the gabbroic sheets, and both phases commonly occur as hybrids (Fig. 3). Much of the northwestern half of the Fraser Zone is dominated by tightly to isoclinally folded, strongly foliated to mylonitic rocks, whereas the least deformed and thickest examples of metagabbroic sheets occur in the southeast, reflecting a significant difference in strain, until the Newman Shear Zone is reached along the eastern boundary of the Fraser Zone (Fig.1). Aeromagnetic and gravity data indicate a repetition of this architecture along strike to the northeast, beneath the Eucla Basin (Fig. 2).

Geochronology of the Fraser Range Metamorphics

Mafic and felsic magmatism was coeval between c. 1310 and c. 1283 Ma (Kirkland et al., 2011a; Spaggiari et al., 2011), and maximum depositional ages of the metasedimentary rocks indicate they were deposited immediately prior to magmatism — 1332 ± 21 Ma for a single zircon analysis, or the more conservative estimate of 1363 ± 9 Ma (MSWD = 1.09) for the 24 youngest analyses (preliminary data from garnet–biotite metasedimentary gneiss, GSWA 194778; see also GSWA 194714, Kirkland et al., 2011c). Magmatic crystallization of two-pyroxene metagabbro from the Fraser Range Black dimension stone quarry in the southeastern part of the Fraser Zone (Fig. 4) has been dated at 1299 ± 3 Ma (GSWA 194717, preliminary data). This date is within uncertainty of interpreted magmatic crystallization dates from two samples of two-pyroxene mafic granulites from southwest of Symons Hill, dated at 1299 ± 10 Ma and 1291 ± 8 Ma (De Waele and Pisarevsky, 2008). It is also identical to a date of 1299 ± 6 Ma from pegmatitic gabbro (GSWA 194782, preliminary data) that intrudes similar metagabbro in the nearby Gold Leaf Black dimension stone quarry (Fig. 4). Near Mount Malcom, pegmatitic gabbro that intrudes metagabbro has a magmatic crystallization age of 1301 ± 6 Ma (GSWA 183653, preliminary data).

The metasedimentary, metagabbroic, and metagranitic rocks record a high-grade metamorphic overprint shortly after formation. For example, zircon rims from garnet–biotite metasedimentary gneiss yield a date of 1298 ± 12 Ma (GSWA 194778, preliminary data), zircon

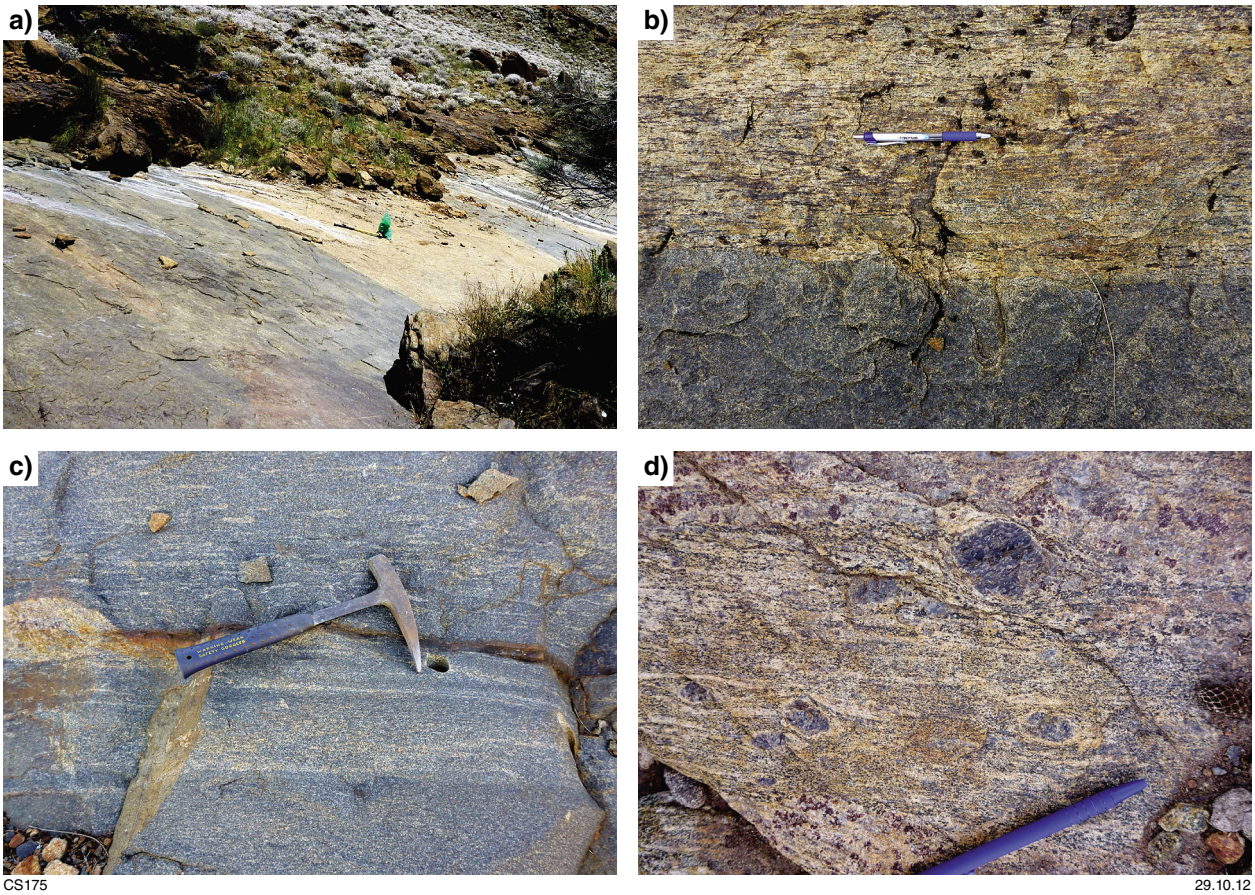

Figure 3. Field photographs of metagabbro, metagranite sheets, and hybrid rocks of the Fraser Zone: a) Metagabbroic rocks (dark) interlayered with sheets of granitic material (pale); Fraser Range Metamorphics, gully exposure at Wyralinu Hill, Fraser Range; b) sheet contact of metagranitic to hybrid rock with metagabbro (darker rock, lower part of photo; gully exposure at Wyralinu Hill, Fraser Range; c) metagabbro with wispy and thin layers of granitic material, and sparse K-feldspar phenocrysts; Phil's Quarry, Fraser Range; d) K-feldspar porphyroclasts in hybrid metagabbroic to metagranitic rocks; Fraser Range Metamorphics, Wyranilu Hill, Fraser Range

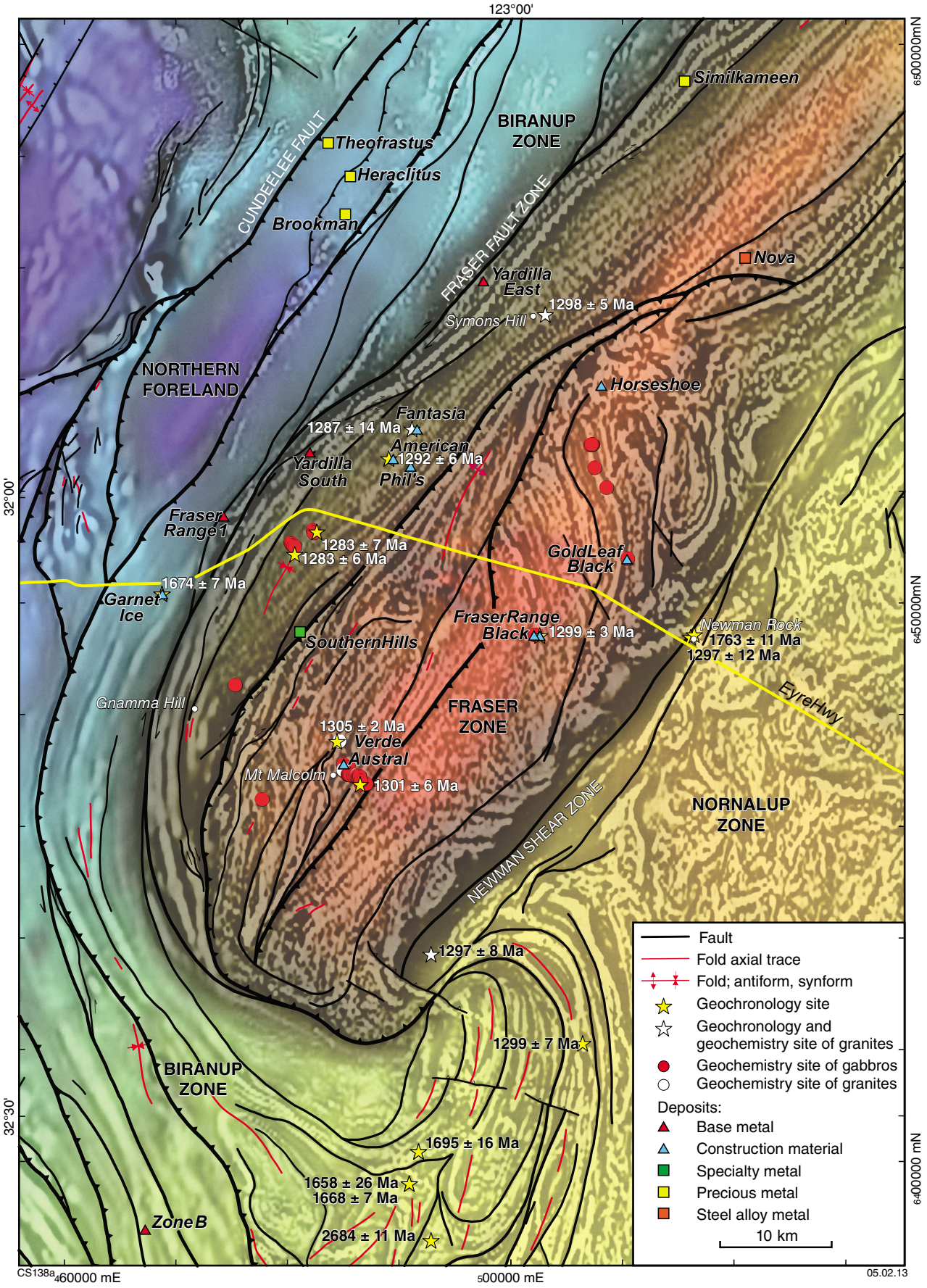

Figure 4. Gravity image with first vertical derivative aeromagnetic drape of the southwestern part of the Fraser Zone, showing major structures, sample locations, and U–Pb (SIMS) ages.

rims from psammitic gneiss yield a date of 1292 ± 5 Ma (GSWA 194714, Kirkland et al., 2011c), and metamorphic zircon from mafic granulite yield a date of 1292 ± 6 Ma (GSWA 194718, Kirkland et al., 2011d). In the psammitic gneiss, metamorphic zircon growth was contemporaneous with in situ melting and leucosome development (GSWA 194715, Kirkland et al., 2011e). Metamorphism has also been constrained at 1304 ± 7 Ma by zircon rim growth within a quartz metasandstone, which also yielded a maximum depositional age of 1466 ± 17 Ma (Wingate and Bodorkos, 2007). A synmetamorphic charnockite from near the Verde Austral Quarry (Fig. 4) has yielded a zircon crystallization age of 1301 ± 6 Ma (Clark et al., 1999), and monazite from granulite facies quartz-rich semipelitic rocks at Gnamma Hill (Fig. 4) yielded ages of 1266 ± 8 Ma (Oorschot, 2011). These dates are interpreted to reflect the age of metamorphism, although not necessarily the time of peak metamorphism. Rubidium–strontium whole-rock biotite ages suggest the Fraser Zone cooled below the biotite closure temperature at c. 1268 Ma (Fletcher et al., 1991). All isotopic results from the Fraser Zone indicate a very short time interval for sediment deposition, igneous crystallization, and near coeval granulite-facies metamorphism. Retrogression, cooling, and uplift occurred shortly after high-grade metamorphism (Fletcher et al., 1991; Clark et al., 1999; De Waele and Pisarevsky, 2008). The close correspondence between the age of mafic to felsic magmatism and the age of granulite facies metamorphism implies magmatism as a thermal driver of metamorphism.

The close relationship between magmatism and metamorphism might be significant in terms of the Ni–Cu sulphide deposit (Nova) recently discovered by Sirius Resources NL at The Eye prospect. This mineralization occurs as pyrrhotite, pentlandite, and chalcopyrite, which display typical magmatic textures including massive, matrix, net-textured, breccia, blebby, and disseminated forms (Sirius Resources NL, 2012a). The host rocks are dominantly gabbroic granulites (Sirius Resources NL, 2012a,b), similar to those described in this Record. Although described as magmatic, the mineralization crosscuts locally garnet-bearing metamorphic layering (Sirius Resources, 2012b). Based on the geochronological data described above, metamorphism occurred shortly after magmatism, and might then have been a significant secondary control on the mineralization. Diamond drillcore of metamorphosed gabbroic to ultramafic rocks that did not intersect the main zone of mineralization (i.e. is structurally above it) contains a non-economic, disseminated sulphide assemblage of pyrrhotite, pentlandite, and chalcopyrite (Gollam, 2012). This is crosscut by lower temperature veins, including serpentinite and talc–carbonate veins (Gollam, 2012), that have colloidal, vuggy, laminated, and brecciated textures. These veins locally contain sulphides, indicating a phase of remobilisation that probably post-dates the main high temperature, ore-forming event.

Previous tectonic models

Several contrasting interpretations for the tectonic setting of the Fraser Zone have been published. Initially, both the metamorphosed granitic and mafic components of the Fraser Zone were interpreted as an exhumed block of lower crust (Doepel, 1975). After detailed mapping, the mafic rocks of the Fraser Zone were then interpreted as part of a large layered mafic intrusion, with the granitic and metasedimentary rocks representing basement slivers (Myers, 1985) belonging to what is now referred to as the Biranup Zone.

Fletcher et al. (1991) examined the Sr-, Nd- and Pb-isotopic composition of the voluminous metamorphosed gabbros of the Fraser Zone and concluded that these rocks were the result of remelting of a mafic underplate and intraplate at c. 1300 Ma. The mafic source was itself derived from a mildly contaminated c. 1900 Ma depleted mantle source with c. 600 Ma of crustal residence.

Condie and Myers (1999) showed that the mafic rocks of the Fraser Zone have the trace element characteristics of subduction-related magmatism. These characteristics are best exemplified on normalized trace element spider diagrams in terms of negative anomalies for Nb and Ta, with respect to other trace elements of similar incompatibility during melting of mantle peridotite. Negative anomalies for Sr and Eu were attributed to subsequent fractionation of feldspar. Condie and Myers (1999) argued that the Fraser Zone represented the remnants of one or more oceanic arcs that were accreted at c. 1300 Ma during closure of a basin separating the Yilgarn and Mawson Cratons. These authors identified five tectonostratigraphic zones of gabbroic rocks, considered to be derived from at least three different subduction-related mantle sources.

More recently, it has been suggested that the gabbroic rocks of the Fraser Zone are the mafic component of a sheeted sill complex (Spaggiari et al., 2011). The gabbros intrude felsic country rock, including metasedimentary rocks deposited shortly prior to gabbro intrusion. The gabbroic rocks are intruded by granitic magmas and in places locally mix with it to produce hybrid mafic to felsic magmas. According to Spaggiari et al. (2011), this sheeted sill complex developed within either a back-arc or rift setting.

The Hf isotopic evolution of the majority of all felsic magmas within the Fraser Zone can be accounted for by normal crustal evolution of a Biranup Zone source (e.g. crustal reworking). However, no region of the Biranup Zone is dominated by solely juvenile signatures. Therefore, a more realistic suggestion is that there was additional radiogenic input into the Fraser Zone, and in fact this is required by geochemical considerations. One analysis from GSWA 194711 (Kirkland et al., 2012), a Recherche Supersuite metamonzogranite from the edge of the Fraser Zone, indicates this point by displaying a significantly more juvenile source with an epsilon value of +5.9. Such a radiogenic Hf composition is probably only a minimum estimate for the degree of juvenile input into the Fraser Zone intrusive rocks as the zircon sample set is strongly dominated by felsic crustal protoliths that yield phases suitable for geochronology. Nonetheless, the Fraser Zone granites are best considered to have Hf isotopic compositions that reflect a degree of juvenile input into a Biranup Zone source. This observation implies

a Biranup Zone basement component to the Fraser Zone (Kirkland et al., 2011b). Such a conclusion is supported by the ages of very rare inherited zircon grains within Fraser Zone granites. These inherited zircon cores range in age from 1770–1604 Ma, similar to the crystallization ages of late Paleoproterozoic magmas within the Biranup Zone. The presence of Paleoproterozoic metagranitic rocks in the Nornalup Zone east of the Fraser Zone (Fig. 1), with ages consistent with the Biranup Zone, further supports the interpretation of a Biranup-like basement component (Spaggiari et al., 2011).

Geochemistry of the Fraser Zone gabbros

Forty-five fine- to medium-grained metamorphosed gabbroic rocks were analysed from the southwestern end of the Fraser Zone, in an area that overlaps that sampled by Condie and Myers (1999) (Fig. 4). The metagabbro samples collected during this project are little affected by recent surface weathering or alteration. For the purpose of identifying the geochemical signatures of any possible contaminant within the gabbro, we complemented our dataset with 70 analyses of granitic units, covering a wide region of the Albany–Fraser Orogen and considered representative of all known major felsic magmatic age groups. The GSWA sample numbers that identify samples used here are listed in Appendix 1, together with location details. All analyses are presented in Appendix 2 and can be obtained from the WACHEM database <http://geochem.dmp.wa.gov.au/geochem/>, together with analytical details.

The gabbros sampled here were broadly divided on the basis of field observations into two groups:

1. Gabbros that show evidence for hybridization or interaction with felsic material (Fig. 3). These were typically sampled close to contacts with granite sheets, although discrete sheets of apparently hybridized gabbros were also found. Distinguishing features of these rocks typically include the presence of subhedral K-feldspar phenocrysts and high and unevenly distributed modal proportions of quartz and K-feldspar, which is commonly developed as stringers or blebs.

2. Gabbros showing no field evidence of any interaction with contemporaneous granites. These were generally sampled from well within individual intrusive sheets.

These groups are identified throughout this Record as ‘hybrid gabbros’ and ‘main gabbros’, respectively. The hybrid gabbros are further subdivided on the basis of geochemistry into Group 1 and Group 2 hybrid gabbros (see later section). Petrographic summaries of these rocks are presented in Appendix 3.

The evolution of relatively primitive magmas like those that produced the gabbros of the Fraser Zone typically involves crystallization of silicate minerals with silica contents similar to those of the bulk magmas. This means that whole rock variations in silica are typically small and are a relatively poor reflection of compositional evolution. Accordingly, major and trace element variations in the gabbros of the Fraser Zone are plotted against $Mg^{\#}$ (molecular MgO/[MgO + total Fe as FeO]), which decreases systematically with compositional evolution. The concentrations of elements that typically are strongly affected by metamorphism and low-temperature alteration (e.g. K, Sr, Ba, Rb), and elements unaffected by such processes (e.g. Zr, Nb), show reasonably well-constrained correlations (Fig. 5), indicating that such processes have not significantly altered the primary compositions of the main gabbros.

Main gabbros

The main gabbros from the various geographical localities (Fig. 4) show significant compositional overlap and typically indistinguishable compositional trends and, accordingly, are likely to be derived from the same, or a similar, source. The rocks show a range in SiO_2 concentrations from 43.0 – 49.9 wt% (Fig. 6). Despite this narrow range, the rocks show a wide range in $Mg^{\#}$ (52–77) and, for all but two samples, $Mg^{\#}$ is negatively correlated with both Fe_2O_3 and TiO_2, indicating an Fe-enrichment trend diagnostic of basaltic rocks of tholeiitic line of descent. The two samples that vary from this trend also have the highest $Mg^{\#}$ (72 and 77), and have anomalously high Fe_2O_3 and low Al_2O_3 and CaO contents. These are particularly olivine-rich samples from weakly layered sheets and are almost certainly cumulates. The presence of these samples indicates that at least some sheets are thick enough to have undergone cumulate processes. Disregarding these two samples, the $Mg^{\#}$ range for the main gabbros is from 52–71 (MgO from 6.9 – 13.1 wt%).

With decreasing $Mg^{\#}$, concentrations of Al_2O_3 decrease slightly but those of all other major element oxides increase, except for CaO, which remains at a relatively constant concentration (Fig. 6). The trends for both Na_2O and Al_2O_3 are subtle. Concentrations of Al_2O_3 remain constant within the $Mg^{\#}$ range from 71 to ~65 and then decrease slightly, whereas concentrations of Na_2O initially increase with decreasing $Mg^{\#}$, but remain relatively constant for $Mg^{\#}$ lower than ~65. The nature of this subtle inflection at $Mg^{\#}$~65 is possibly consistent with late crystallization of feldspar. Although rather scattered, the data for K_2O and P_2O_5 show the greatest increases in concentration, both increasing by a factor of ~4.

Apart from the two high-$Mg^{\#}$ cumulate samples, the main gabbros show only slight decreases in Cr concentrations (~680–160 ppm) with decreasing $Mg^{\#}$, but show much more systematic decreases in the concentrations of Ni (~470–75 ppm) (Fig. 7). As with Na_2O, there is a slight inflection in the trend for Cr, with concentrations remaining rather constant at $Mg^{\#}$ below ~65.

The large ion lithophile elements (LILE; Sr, Ba) show significant increases in concentration with decreasing $Mg^{\#}$, except for Sr, which initially shows a slight increase in concentration, but then remains at relatively constant concentrations (Fig. 7).

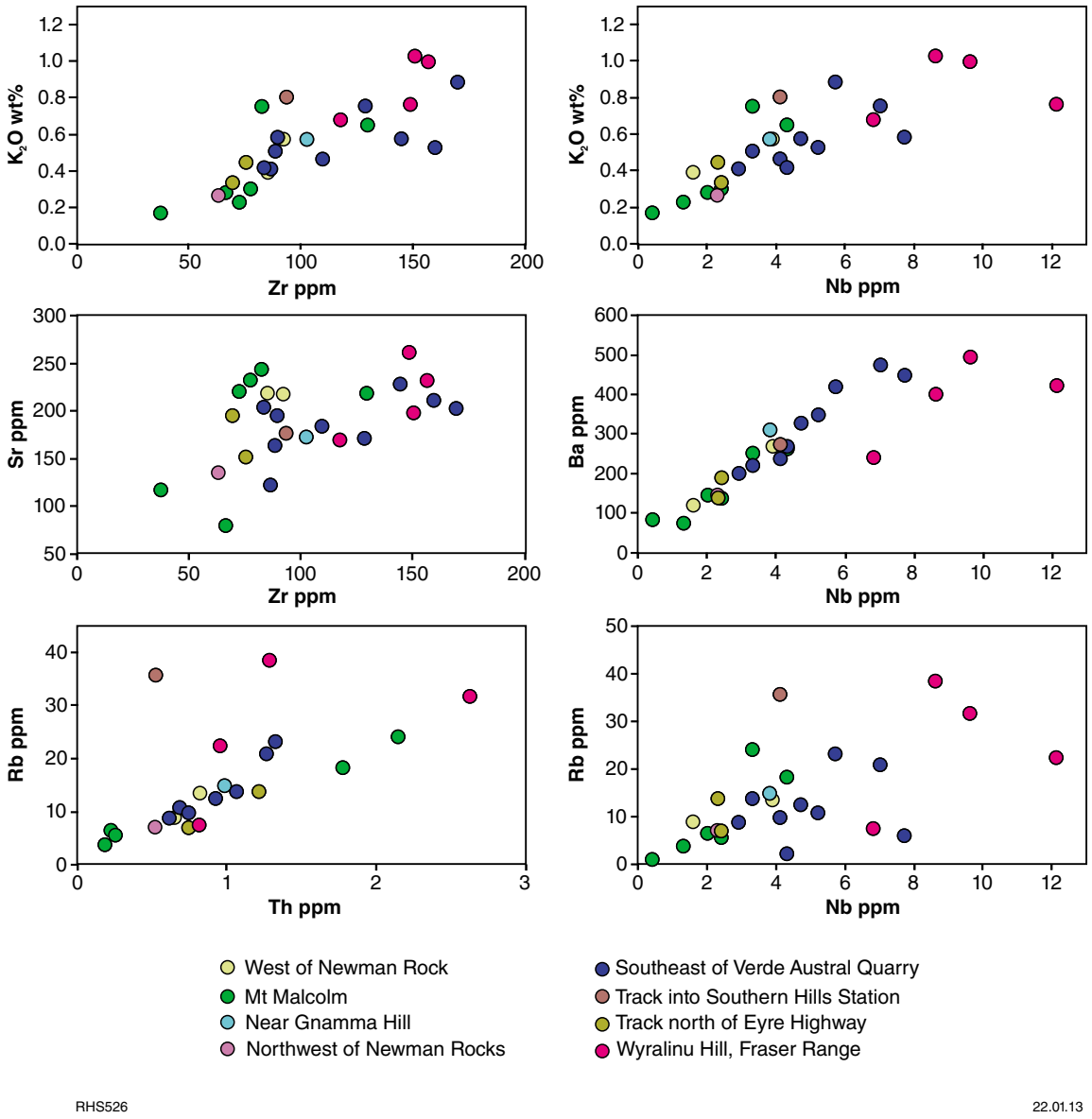

Figure 5. Compositional variation diagrams showing correlations between fluid-mobile elements K, Sr, Ba, and Rb and fluid-immobile elements Zr, Nb, and Th, for gabbros that show no field evidence for hybridization (main gabbros).

Concentrations of Th, U, Nb, Ta, Zr, Hf, and rare earth elements (REE) increase with decreasing $Mg^{\#}$, although the data are very scattered (Fig. 7; Zr, Hf, REE not shown). Some of the scatter can be attributed to three samples in particular — two samples from Mount Malcom and one sample from Near Newman Rocks (GSWA 183624, 183654, 183665) — which, at moderate $Mg^{\#}$ (58–63), are notably depleted in most incompatible trace elements. Incompatible trace element ratios, typically strongly correlated with magmatic compositional evolution (e.g. La/Sm, La/Yb, Nb/Zr), also show increases with decreasing $Mg^{\#}$, again with the exception of the same three outliers.

Compared to MORB (Fig. 8), the most primitive samples of main gabbros (excluding the cumulate samples) are strongly enriched in LILE and light rare earth elements (LREE), have MORB-like concentrations of Nb (and Ta), Zr, and Hf, and are notably depleted in heavy rare earth elements (HREE). On a MORB-normalized trace element spidergram, the three samples with apparently anomalously low incompatible trace element concentrations (GSWA 183624, 183654, 183665 – red lines on Figure 8) show trace element patterns distinctly different from the typically enriched patterns shown by the other rocks. These three samples were clearly derived from a source that was significantly more depleted, via a previous mantle melting event, than MORB-source or the mantle source component for the other main gabbros. The presence of more than one mantle source component to

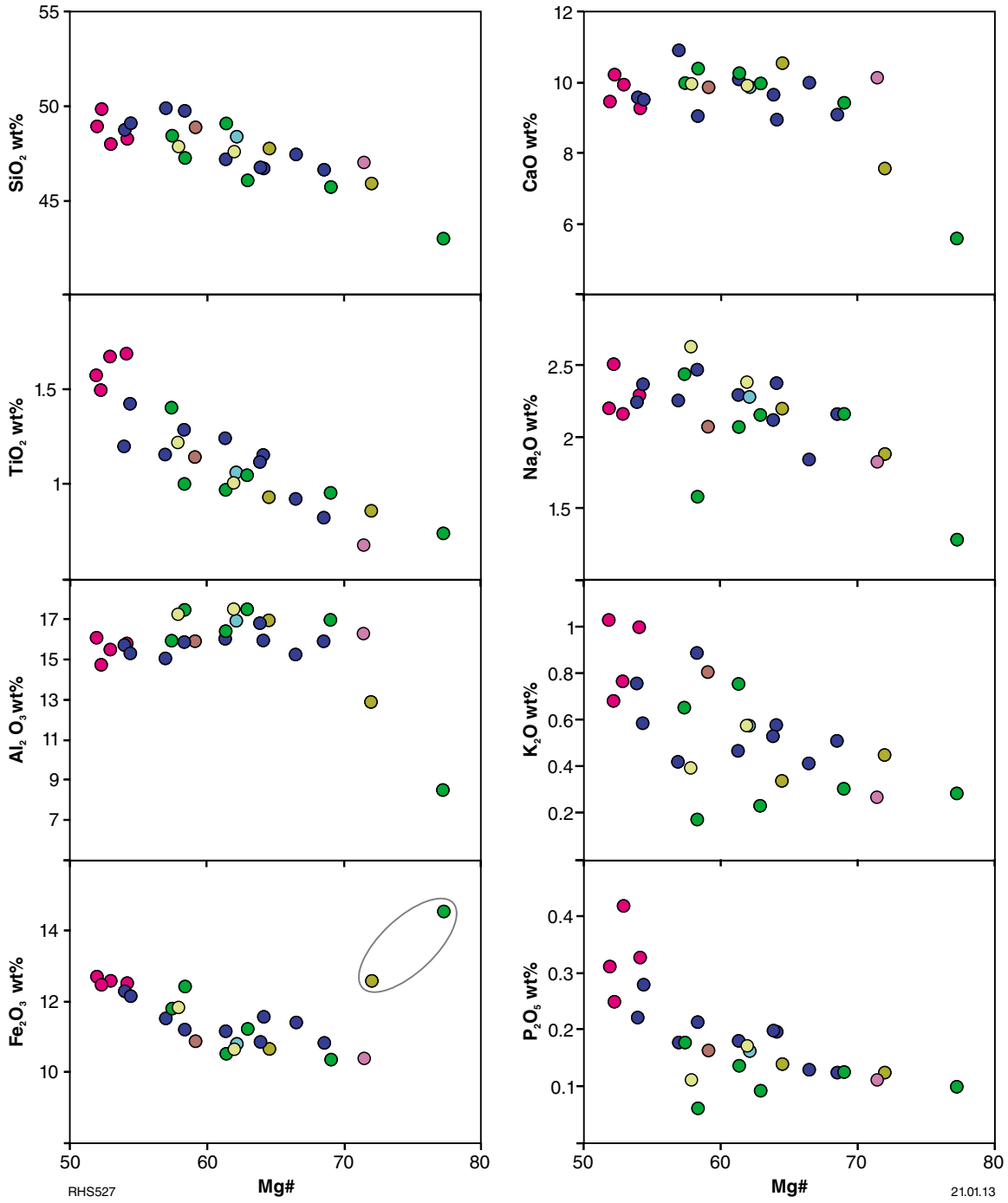

Figure 6. **Compositional variation diagrams showing major element variations against Mg# for gabbros that show no field evidence for hybridization (main gabbros). Two high-Mg# cumulates are identified (circled) on the Fe_2O_3 versus Mg# plot. Symbols as for Figure 5.**

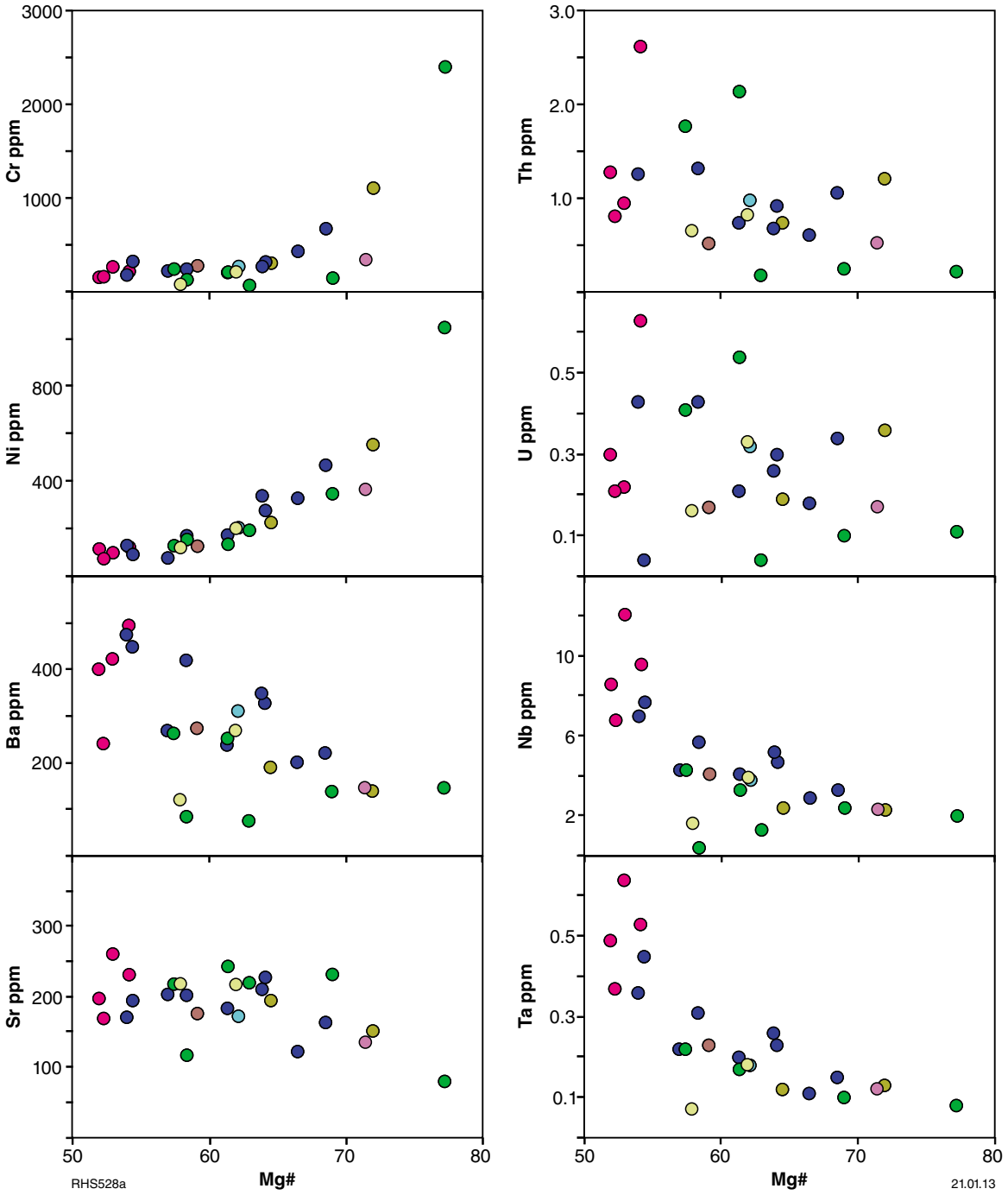

Figure 7. **Compositional variation diagrams showing variations in the concentrations of selected trace elements against $Mg^{\#}$ for gabbros that show no field evidence for hybridization (main gabbros). Symbols as for Figure 5.**

the gabbros of the Fraser Zone was also noted by Condie and Myers (1999), although it is clear from our data that magmas resulting from these discrete source regions are not restricted to distinct geographical zones.

Hybrid gabbros

The interpretation that specific gabbros have incorporated felsic material (e.g. by assimilation or magma mixing) can be readily made in the field and is supported by geochemistry. Although there is a degree of overlap, compared to the main gabbros, the field for hybrid gabbros is displaced to higher SiO_2 concentrations and lower $Mg^{\#}$ (Fig. 9). Trends for a range of incompatible trace elements typically parallel the trends defined by the main gabbros, but with greater scatter in the data.

In detail, two discrete groups of hybrid gabbros can be identified (Fig. 9). The first (Group 1), typically overlaps the high-SiO_2, low-$Mg^{\#}$ part of the field for the main gabbros and shows a similar range in concentration for most incompatible trace elements. The second group (Group 2) shows more significant increases in SiO_2 and decreases in $Mg^{\#}$ compared to both Group 1 and the main gabbros, and also shows significant increases in the concentrations of most incompatible trace elements. The distinction between these two groups, and the main gabbros, is best seen on a plot of Th versus La (Fig. 9), in which Group 1 hybrid gabbros define a discrete low-La trend and Group 2 hybrid gabbros define a discrete high-La trend, whereas the main gabbros lie between the two. Importantly, both groups are found at most of the sites that were sampled during this study and so both reflect processes intrinsic to emplacement of the Fraser Zone gabbros.

Petrogenesis of the Fraser Zone gabbros

Main gabbros

The most primitive samples of main gabbros (excluding the cumulate samples – GSWA 183652 and 183669) have Th, U, and REE concentrations similar to EMORB (enriched mid-ocean ridge basalt), but are significantly depleted in Nb and Ta compared with EMORB and plume-related magmas. Initial MORB-normalized depletions in HREE in many of the main gabbros might reflect a garnet-bearing residue in the source. Slight depletions in HREE might also be expected with higher degrees of mantle partial melting than is typical for the formation of MORB (e.g. Jolly et al., 2001). Alternatively, these depletions might indicate a previously melt-depleted source (more depleted than MORB-source), as suggested above for samples GSWA 183624, 183654, and 183665.

Jolly et al. (2001) used concentrations of Nb and Yb in basalt, corrected to 9.0 wt% MgO (i.e. concentration of Nb and Yb projected to 9.0 wt% MgO along MgO versus Nb and Yb population trendlines), to estimate the degree of mantle partial melting. Using this grid, formation of the parental melts to the main gabbros of the Fraser Zone could be achieved through <10% partial melting of a non-garnetiferous spinel lherzolite. This figure is possibly slightly low considering the rather high MgO content (>13wt%) and moderate $Mg^{\#}$ (up to 71 in non-cumulate rocks) in some of these rocks. However, the low concentrations of Cr in the most primitive main gabbros (<700 ppm) suggest that clinopyroxene remained in the mantle source after melting. This would limit the degree

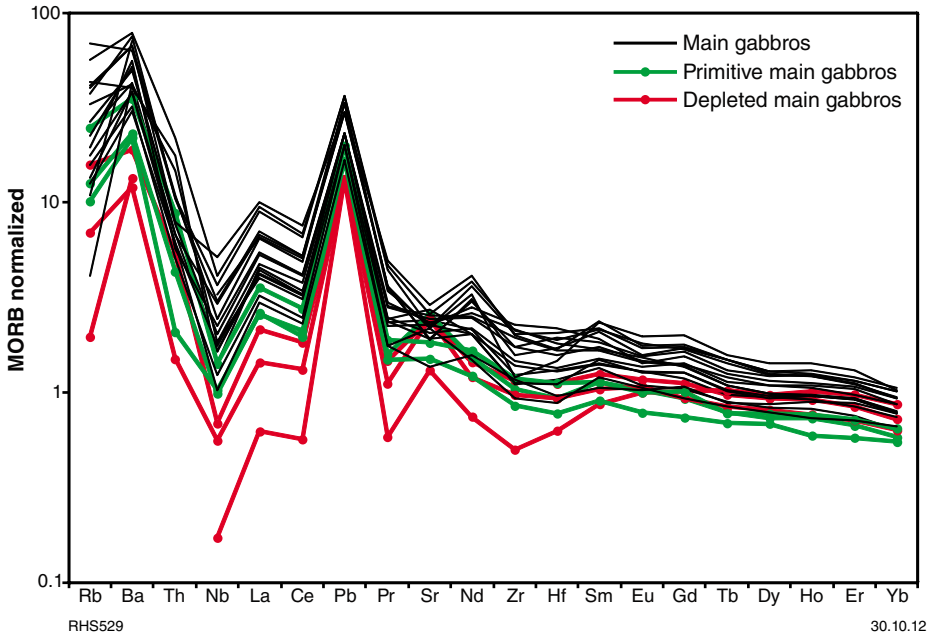

Figure 8. MORB-normalized incompatible trace element spidergrams for gabbros that show no field evidence for hybridization (main gabbros). Normalizations after Sun and McDonough (1989).

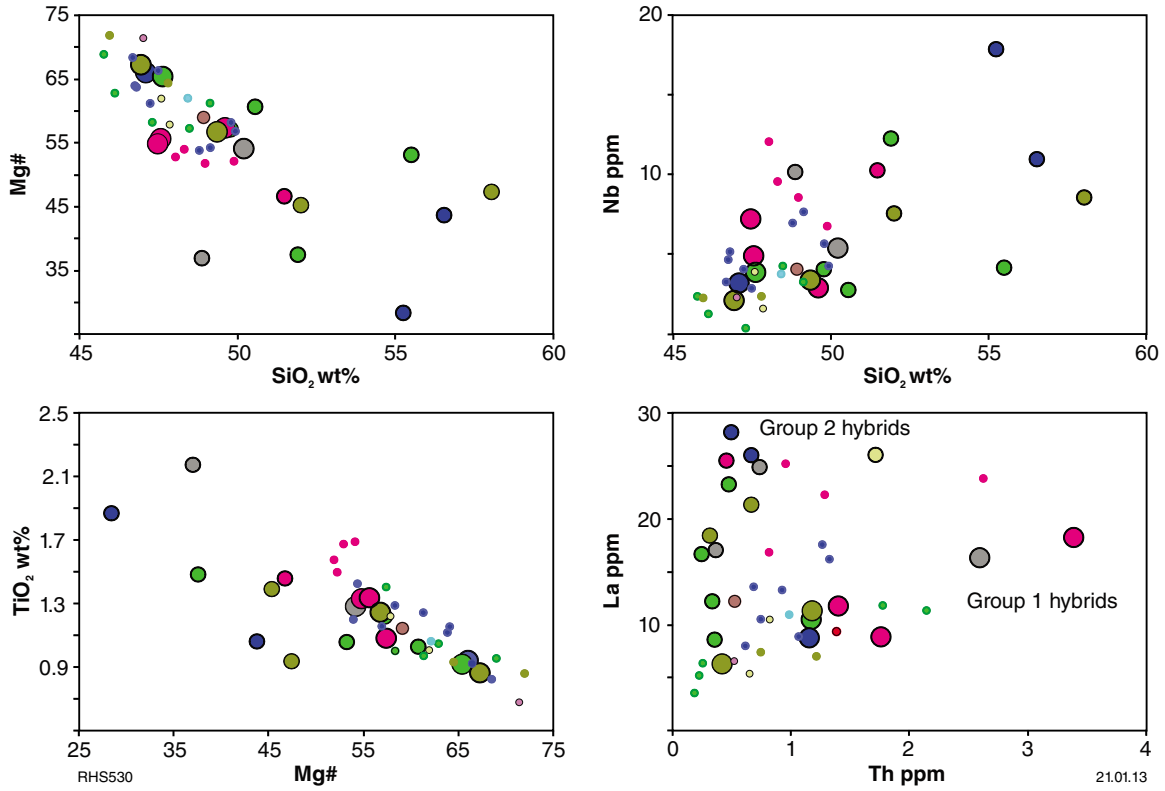

Figure 9. Compositional variation diagrams showing the distinction between main gabbros and hybridized gabbros. Symbol colours as for Figure 5 with the addition of grey symbols for samples taken from the Verde Austral Quarry. Large symbols denote Group 1 hybrid gabbros, medium-sized symbols denote Group 2 hybrid gabbros, small symbols denote main gabbros.

of melting to well below 20% (e.g. Sinton et al., 2003). Hence, the low HREE concentrations in many of these rocks are probably not entirely attributable to high degrees of mantle melting. A source more depleted than MORB-source is already indicated by three of the gabbro samples, and it is tempting to suggest that this is, at least partially, the cause of the low HREE in the other samples.

Regardless of the origins of the HREE depletions in the most primitive main gabbros, at such high $Mg^{\#}$ (i.e. >65), the accompanying enrichments in (for example) Th and LREE cannot be a result of fractional crystallization alone, but reflect either an enriched source or crustal assimilation. These kinds of trace element patterns are characteristic of subduction-related magmas, in which LILE [>Light REE (e.g. La, Ce) >Middle REE (e.g. Sm, Gd)] are preferentially enriched compared to high field strength elements (HFSE) and HREE in the mantle source, depending to some extent on whether both slab fluids and melts are involved. Such patterns formed the basis for interpreting the gabbros of the Fraser Zone as the remnants of one or more oceanic arcs (Condie and Myers, 1999). However, the same trace element patterns can result through assimilation of crustal material into ascending mantle-derived magmas. Recent geological and geochronological data from the Albany–Fraser Orogen appear to favour formation of the Fraser Zone in a distal back-arc rift or an intracratonic rift setting (Spaggiari et al., 2011; Oorschot, 2011; Clark et al., in prep). Hence, establishing how the main gabbros acquired their enriched geochemical signature can provide important constraints on the environment in which the rocks evolved.

Using a compositionally similar data set to that discussed here, Condie and Myers (1999) dismissed any suggestion that subduction-like features in the gabbros of the Fraser Zone were inherited through assimilation of crustal rocks because the major element and Ni contents of the gabbros do not allow for significant assimilation, and because the isotopic composition of the gabbro is 'relatively juvenile'. However, Fletcher et al. (1991) had already established that the Sr-, Nd-, and Pb-isotopic composition of these rocks required a bulk source with a weighted average crustal residence of c. 600 Ma. This almost certainly excludes formation in an oceanic arc environment.

Condie and Myers (1999) also noted distinct trace element patterns in gabbros of the Fraser Zone, including a melt-depleted source. They related these to a range of different mantle source components, individually feeding separate lithotectonic units interpreted to reflect fragments of separate oceanic arcs. Our data do not appear to require more than one mantle source component (slightly depleted mantle). Even if the three depleted samples are interpreted to derive from a unique source, it is clear that magmas resulting from these potentially discrete source regions

are not restricted to particular geographical zones. Hence, the compositionally discrete source regions suggested by Condie and Myers (1999) would be geographically overlapping. Regardless of how many mantle source regions might be involved, the evidence presented here, that all sources were melt depleted, means that LILE and LREE variations, and ratios involving these trace elements, will effectively be controlled by the composition of the enriching component.

Although the incompatible trace element enriched patterns of the main gabbros are generally typical of subduction-related magmas, the observed enrichments in LILE do not include systematic enrichments in Sr (Fig. 8). In fact, for most samples, normalized Pr/Sr and Nd/Sr ratios are <1 (i.e. they have a negative Sr anomaly on normalized trace element spidergrams). Condie and Myers (1999) also noted that the gabbros of the Fraser Zone had negative Sr and Eu anomalies and attributed these features to subsequent fractionation of plagioclase in a subduction-related mafic magma. However, such decoupling of Sr from the other LILE is typically not observed in subduction-related magmas. Rocks in the compositional range of basalt, from a range of subduction environments, characteristically show strong positive normalized Sr anomalies (Fig. 10), reflecting the high mobility of Sr in fluids leaving subducting slabs and the instability of plagioclase during slab-melting. Subduction-derived magmas are also typically hydrous, which inhibits early plagioclase crystallization and further promotes Sr concentration within the melts.

Whereas removal of plagioclase from a crystallizing magma will cause depletions in Sr, variations in Sr and Eu/Eu* in the main gabbros are not correlated with $Mg^{\#}$ (e.g. $Mg^{\#}$ versus Sr, Fig. 7), so plagioclase fractionation is not the cause of the Sr depletions. Thus, these depletions are most likely an intrinsic feature of the magmas and are probably not a result of subduction-related processes.

Accordingly, we need to assess the suggestion that assimilation of basement cannot explain the compositional evolution of the gabbros of the Fraser Zone (Condie and Myers, 1999). To do this, the composition of the main gabbros was compared with available crustal components (granites and felsic orthogneiss) throughout the Albany–Fraser Orogen. In making such assessments, it is important to determine at what stage in magmatic evolution any potential assimilation might occur. Early assimilation, followed by isolation and subsequent closed-system fractionation, can have a significantly different effect on compositional evolution than continuous or late assimilation. Simple binary mixing models (Fig. 11) immediately discount the (inherently unlikely) possibility that mixing of any regionally available felsic component into a primitive gabbro can, on its own, explain the evolved compositions of the remaining main gabbros. Indeed, these models effectively constrain the amount of crustal material that could be involved, in any scenario, to a maximum of ~5%. Bulk assimilation of a greater amount of felsic crust would lead to gabbros with much higher concentrations of SiO_2 and K_2O than observed.

The most primitive main gabbros have La/Nb ratios ~2.7, notably higher than primitive mantle values of ~1.0 (Sun and McDonough, 1989). These ratios, however, decrease slightly with decreasing $Mg^{\#}$ (Fig. 12), reflecting fractional crystallization of normal 'basaltic' silicates (e.g. olivine and pyroxene) with very limited, or no, subsequent interaction with crustal material. Thus, any potential assimilation or contamination must have occurred very early — either at the source or in

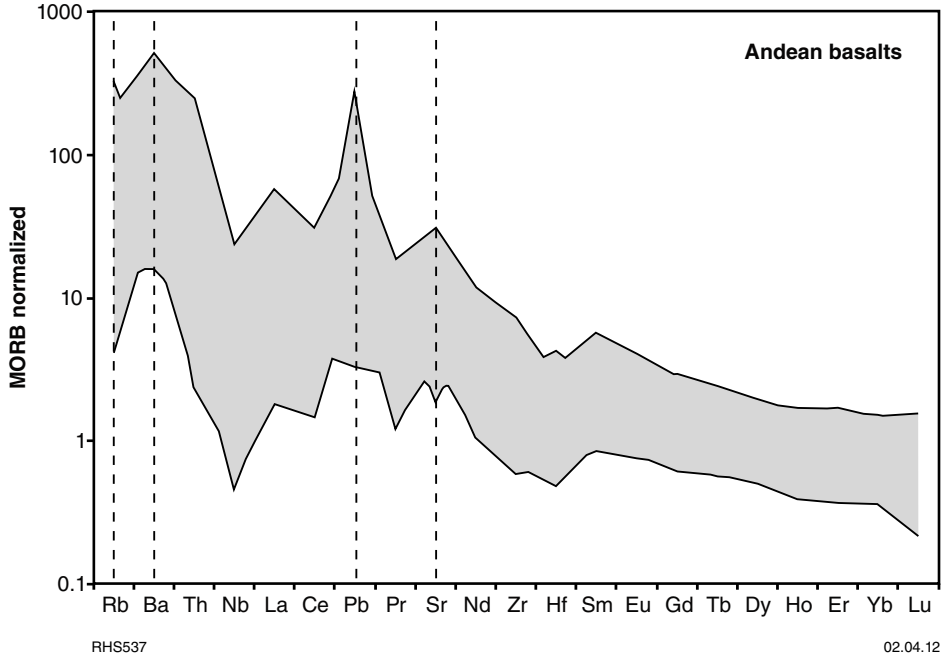

Figure 10. MORB-normalized incompatible trace element spidergrams for basalts from a range of continental arc settings. Data from the GEOROC database <http://georoc.mpch-mainz.gwdg.de/georoc>. Normalizations after Sun and McDonough (1989).

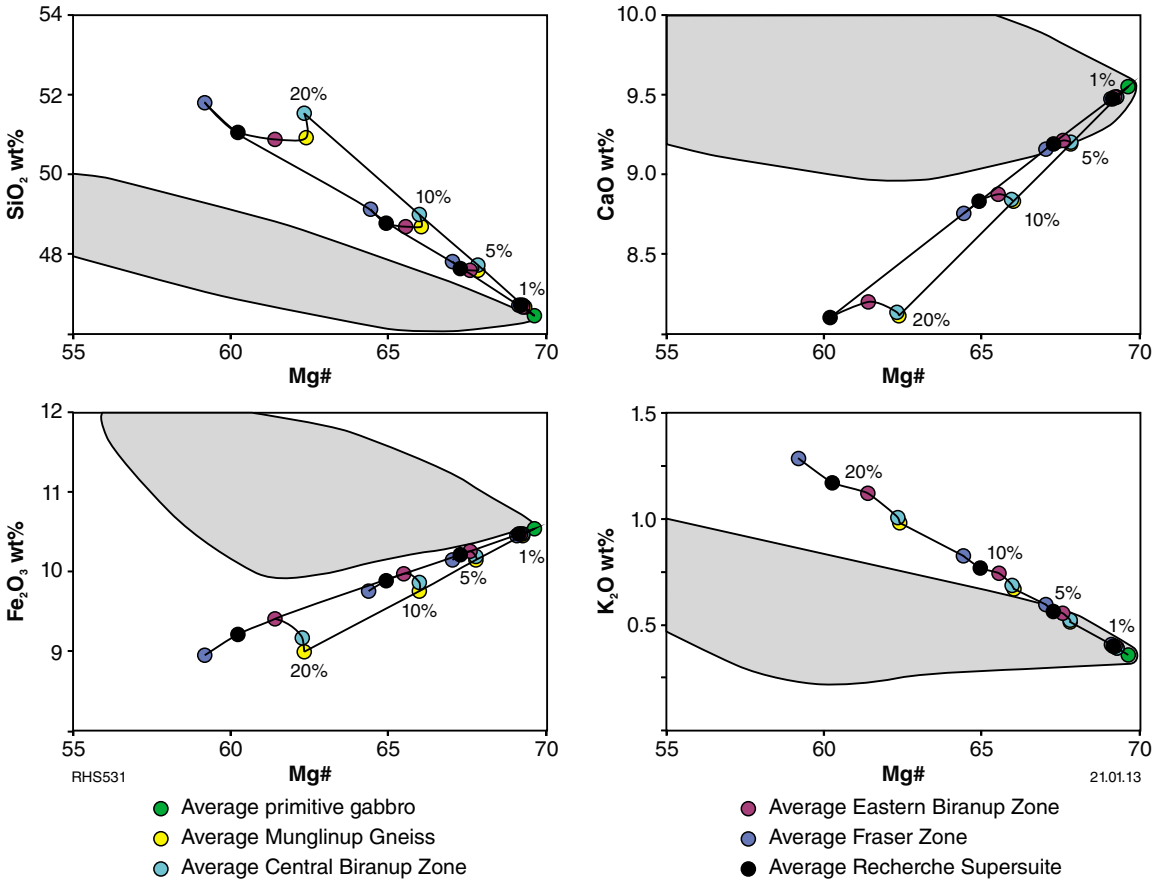

Figure 11. Compositional variation diagram showing the effects of simple binary mixing of 1%, 5%, 10%, and 20% of various potentially available felsic crustal components into a magma with the composition of a primitive Fraser Zone main gabbro. The grey field encloses all analyses of main gabbros.

lower-crustal staging chambers — and all subsequent compositional evolution was purely a result of closed system fractional crystallization. Figure 13 shows the effects on trace element concentrations of assimilating available Albany–Fraser Orogen crustal components into a magma with MORB-like composition. It is immediately apparent that even very minor amounts of assimilation of felsic crust essentially establish the incompatible trace element patterns. Any incompatible trace element enrichments caused by early assimilation will be greatly accentuated through fractional crystallization, and so the amount of assimilation required to produce the observed trace element patterns in the main gabbros will be greatly reduced.

Figure 14 plots the results of trace element modelling. The purpose of this modelling was to test if assimilation of available Albany–Fraser Orogen crustal components into a mantle-derived melt, followed by fractional crystallization, can result in normalized incompatible trace element patterns similar to those of the Fraser Zone gabbros. Note that it is primarily the relative concentrations of the trace elements (i.e. the 'shape' of the normalized patterns) rather than the absolute concentrations that are important here. For the gabbros, this shape does not

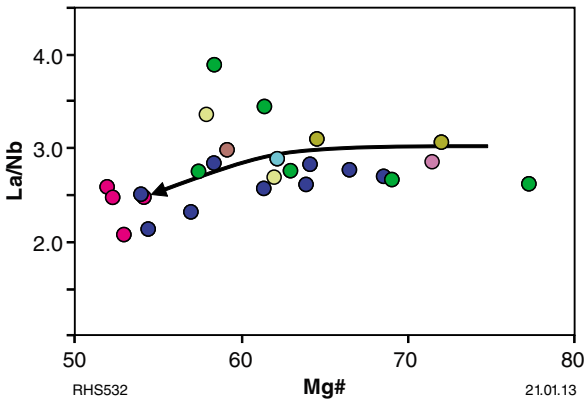

Figure 12. Compositional variation diagrams showing variations in La/Nb ratio against Mg# for gabbros that show no field evidence for hybridization (main gabbros). Symbols as for Figure 5.

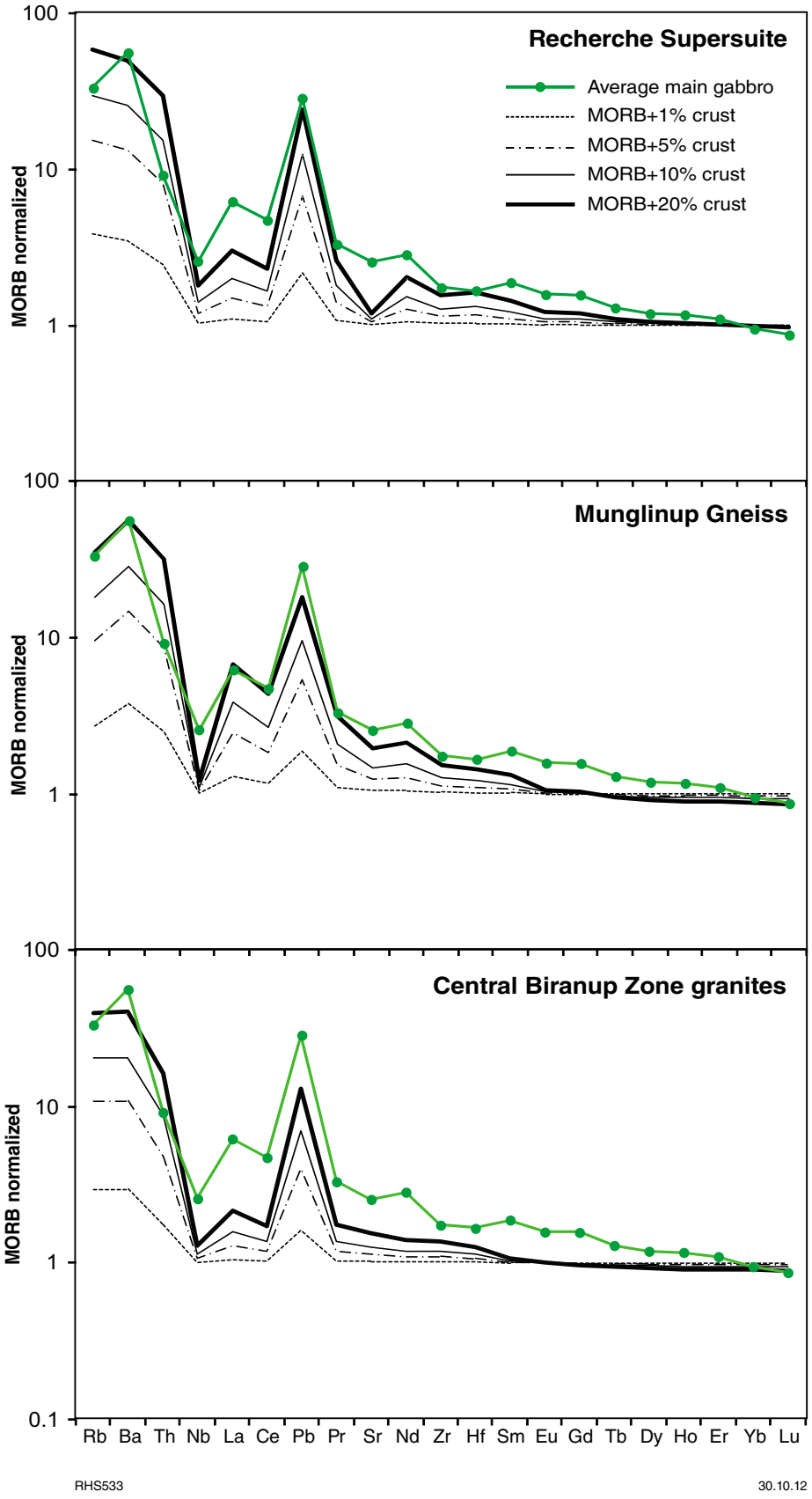

Figure 13. MORB-normalized incompatible trace element spidergram modelling the effects of assimilating various potentially available felsic crustal components into a magma with MORB-like composition. The average composition of the main gabbros is shown for comparison.

change significantly with decreasing $Mg^{\#}$, so the results are compared to an average gabbro composition. Two mantle melt compositions were tested — MORB and an even more depleted hypothetical composition, which is represented on a MORB-normalized trace element spidergram by a line extrapolated between the elements Yb, Zr, and Nb (the incompatible trace elements least enriched through crustal interaction) for the most depleted gabbro sample (Fig. 15). To model assimilation of basement, 10% locally available crustal material was added to each of these melt compositions. Crustal material used included: average Munglinup Gneiss (Northern Foreland, reworked Archean Yilgarn Craton); average Paleoproterozoic granite from the central and eastern part of the Biranup Zone; average Mesoproterozoic Recherche Supersuite granite; and the average of Archean high-Ca granites from the Kalgoorlie Terrane (David Champion – written communication, 2011).

Fractional crystallization of each of these contaminated melts was then modelled using average values for distribution coefficients quoted in the GERM database <http://earthref.org/GERM> to produce bulk distribution coefficients for a range of hypothetical fractionating assemblages incorporating various combinations of pyroxene, olivine, and garnet. Assumed values for F (amount of liquid remaining during fractionation) were 0.5 (i.e. 50% crystallization) and 0.25 (75% crystallization). Although the binary mixing models show 10% assimilation to be a maximum value, values significantly lower than this would have produced weakly contaminated melts that required degrees of subsequent fractional crystallization that were unrealistically high (F <0.25), given the major element compositions of the main gabbros themselves. This observation itself might indicate that any viable basement component assimilated into the gabbroic melts was mafic to intermediate, rather than strongly felsic. Alternatively, it may relate to the fact that the modelling presented here reflects simple bulk assimilation of basement rock, rather than the more realistic (but considerably harder to constrain) case of assimilation of (or mixing with) low-degree partial melts of basement rocks. The primary difference between the two will be in the significantly higher concentration of the more highly incompatible trace elements during the latter process.

Immediately clear from the trace element models is that, irrespective of the chosen assimilated material, any potential fractionating assemblage must have included garnet in order to reproduce the fractionated MREE–HREE normalized patterns seen in the main gabbros (Fig. 14). Although we can only model the influence of garnet by assuming this mineral formed part of the assemblage fractionating from the contaminated melt, it is equally (or perhaps more) likely that the fractionated MREE–HREE patterns for the gabbros are a result of residual garnet in the source of either the mantle melt component or the crustal (assimilated) component. This is probably why trace element models using average Archean high-Ca tonalite–trondhjemite, or reworked Archean granite (i.e. the Munglinup Gneiss), provide the best match with the main gabbros.

Whereas most of the models produce trace element patterns that resemble those of the main gabbros (Fig. 14), most of the models also require high degrees of fractional crystallization (F ~0.25), particularly for the highly incompatible trace elements and where the assumed mantle melt component was more depleted than MORB. In addition, only models that assumed assimilation of average Munglinup Gneiss, granite from the eastern part of the Biranup Zone, or average Recherche Supersuite granite result in patterns that reproduce the slight negative Sr anomalies seen in the gabbros. Similarly, only the average Archean high-Ca tonalite–trondhjemite, and the average of the three most mafic granites of the eastern Biranup Zone, are depleted enough in Th to explain the Th concentrations in the gabbros.

The most reasonable matches with the observed trace element patterns in the gabbros are obtained either (i) by using a MORB-like mantle component and the mafic granites of the eastern Biranup Zone, or (ii) by assuming a mantle melt only slightly more depleted than MORB (i.e. compositionally between MORB and the depleted mantle melt modelled in Figure 15) and a crustal component transitional between average Archean high-Ca tonalite–trondhjemite and Munglinup Gneiss (Fig. 14). Given that the Munglinup Gneiss is itself reworked Archean granite, either of these two latter models seems very reasonable. Thus, within the modelling limits available, it appears quite possible that assimilation of available basement can explain the compositional evolution of the main gabbros of the Fraser Zone. Given the existing Nd- and Hf-isotopic signatures, this is most likely a more viable model than invoking a subduction-modified mantle source (cf. Condie and Myers, 1999). The suggestion that the assimilated basement was Archean granite or reworked Archean granite obviously has significant implications in terms of crustal architecture.

Hybrid gabbros

The observation that the two groups of hybrid gabbros form distinct high- and low-La trends that effectively envelope the field for the main gabbros (Fig. 9), suggests the two hybrid groups formed through two distinct and unrelated processes. It is also clear, both from field observation and from the typically higher $Mg^{\#}$ in the main gabbros, that the main gabbros do not simply represent mixes between the two hybrid groups. Another critical point is that, whatever the process forming the two hybrid groups, examples of each group are found at all sites sampled during this study, so the petrogenetic processes involved are not isolated phenomena.

In terms of their variations in Th and La, the trends for both Group 1 and Group 2 hybrid gabbros can possibly be explained simply in terms of fractional crystallization of slightly different parental compositions. In general, Group 2 rocks appear to be considerably more fractionated, with a significant range in $Mg^{\#}$ (61–28) and SiO_2 (48.8 – 58 wt%) compared to Group 1 ($Mg^{\#}$ = 67 to 54; SiO_2 = 46.9 to 50.2 wt%). However, this model would require three distinct parental magmas — all present at all localities.

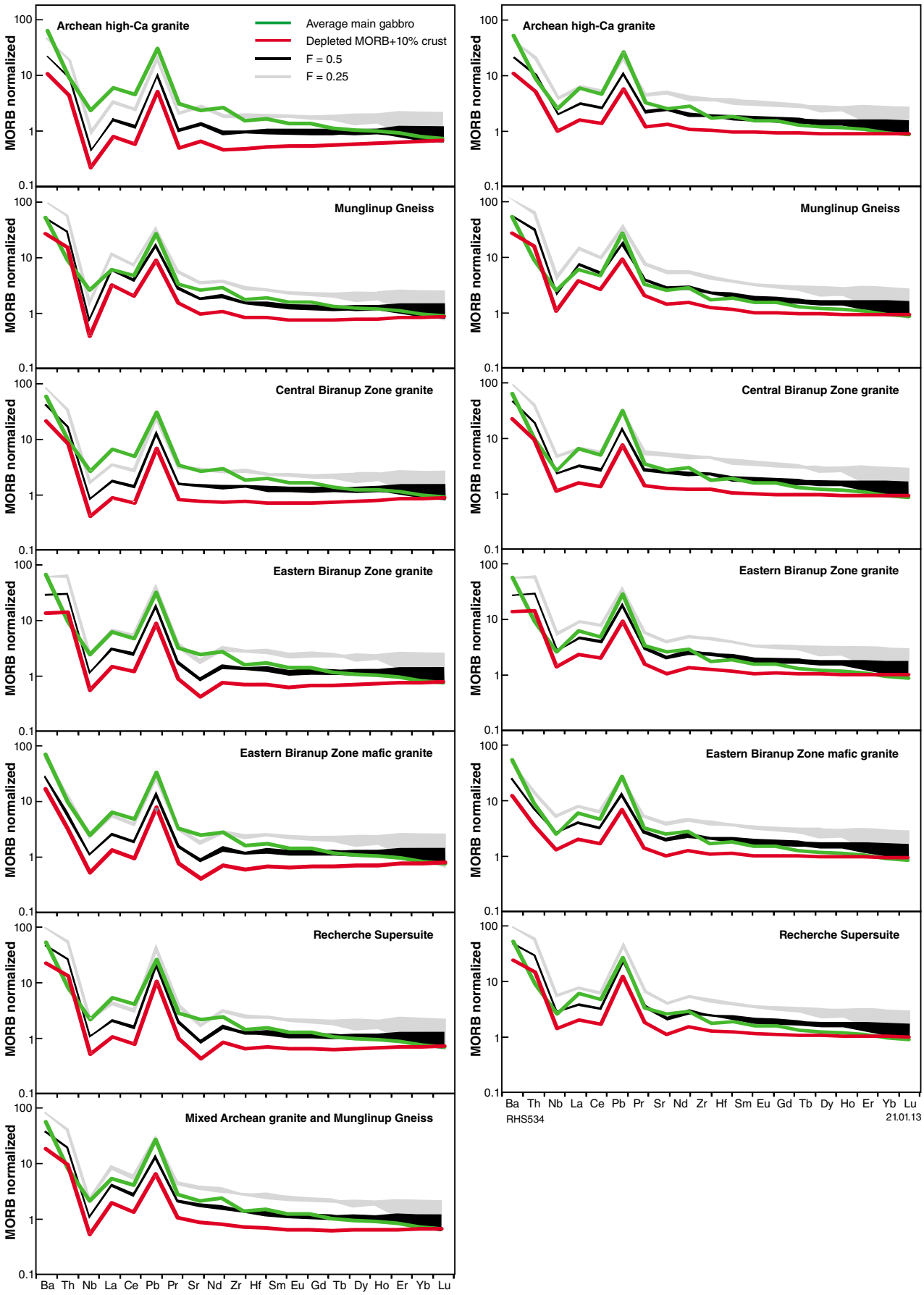
Archean high-Ca granite
Average main gabbro
Depleted MORB+10% crust
F = 0.5
F = 0.25
Munglinup Gneiss
Central Biranup Zone granite
Eastern Biranup Zone granite
Eastern Biranup Zone mafic granite
Recherche Supersuite
Mixed Archean granite and Munglinup Gneiss
MORB normalized
100
10
1
0.1
Ba Th Nb La Ce Pb Pr Sr Nd Zr Hf Sm Eu Gd Tb Dy Ho Er Yb Lu
RHS534
21.01.13

Figure 14. (facing page) MORB-normalized incompatible trace element spidergrams showing the results of trace element modelling (see text for details). Two mantle melt compositions — MORB (right column) and a melt derived from a source more depleted than MORB-source (left column) – see Figure 15 — are contaminated by addition of various potentially available felsic crustal components prior to fractional (Rayleigh) crystallization of a range of mineral assemblages for values of F (proportion of melt remaining) of 0.5 and 0.25. Mineral melt distribution coefficients are average values for clinopyroxene (cpx), orthopyroxene (opx), olivine (ol) and garnet (gnt) in basaltic magmas and are taken from the GERM website <http://earthref.org/GERM>. Bulk distribution coefficients for five hypothetical fractionating assemblages are based on the following proportions of cpx:opx:ol:gnt: A) 0.5:0.25:0.25:0; B) 1.0:0:0:0; C) 0.7:0.15:0:0.15; D) 0.4:0.2:0.25:0.15; E) 0.85:0:0:0.15. Results for each value of F for all five hypothetical fractionating assemblages are grouped into shaded single fields. For each field, the garnet-bearing assemblages define the low MREE–HREE end of the range. The average composition of the main gabbros is shown for comparison. Normalizations after Sun and McDonough (1989).

The trend of Group 1 hybrid gabbros, in most compositional variation diagrams, is towards the composition of high-Th monzogranite sheets sampled at several localities (Fig. 16). Indeed, most of the compositional variation in Group 1 hybrid gabbros can be explained by incorporation of up to 30% of this granite into main gabbro magmas. These granites are locally interleaved with the Fraser Zone metagabbros and have crystallization ages (1298 ± 5 Ma, GSWA 194719) equivalent to those of the main gabbros themselves. They form locally voluminous intrusions, typically of highly leucocratic and schlieric garnet-bearing metasyenogranite, and are compositionally similar to other samples of the Recherche Supersuite taken from throughout the Fraser Zone and the Nornalup Zone to the southeast. Note that direct incorporation of this granite melt into a mantle derived melt cannot be the reason for incompatible trace element enrichments in the main gabbros (see above) because the granites are too enriched in Th and have Th/La ratios that are too high. However, incorporation of these granites into the main gabbro melt during ascent or emplacement of the gabbro appears to be a viable model for Group 1 hybrid gabbros.

The relationship between Group 2 hybrid rocks and the main gabbros is intriguing. The high-SiO_2, low-$Mg^{\#}$ hybrids cannot be parental to the main gabbros, and the reverse relationship cannot be true through fractional crystallization alone, because the hybrids have lower Th concentrations. Fractional crystallization of basaltic compositions normally will not lead to greater relative increases in the concentrations of La compared to Th. Even if we assume that both elements are perfectly incompatible during fractional crystallization, the most primitive main gabbro should still evolve La/Th ratios much lower than those of Group 2 hybrid gabbros. As with the Group 1 hybrid gabbros, because Group 2 hybrid gabbros are found at all sampled localities, it is likely that their petrogenesis is directly related to intrusion of the main gabbro sheets and the formation of the sheeted sill complex in general. In the case of the Group 1 hybrid gabbros, mixing with locally and regionally available contemporaneous leucosyenogranite magmas of the Recherche Supersuite provides a viable petrogenetic model, but these granites are too Th-rich and Ba-poor to be involved in the formation of the Group 2 hybrid gabbros (Fig. 16).

However, granite melt sheets comagmatic with the gabbros fall into two broad compositional groups — the first of which is the garnet-bearing leucosyenogranites. The second group of granites comprises sheets and other small intrusive bodies of very K_2O-rich and incompatible trace element depleted leucogranites (Fig. 16). These depleted leucogranites represent the only currently known felsic material with high enough La/Th ratios to produce compositions similar to those of Group 2 hybrid gabbros, when mixed with main gabbro. The unusually depleted and high-K compositions of the granites almost certainly reflects very low-degree, modal melting of sedimentary rocks under disequilibrium conditions where incompatible trace element rich accessory phases (e.g. zircon, apatite, monazite) are either shielded within refractory minerals or are metastable. Thus, Group 2 hybrid gabbros likely represent assimilation, at the level of the sill complex, of low-degree melts of the metasedimentary country rocks.

On incompatible trace element variation diagrams, data for the main gabbros tend to scatter between the well constrained fields for the two hybrid gabbro groups. As discussed above, the incompatible trace element enriched compositions of the main gabbros appear to be the result of assimilation of basement material, before emplacement, and cannot be a result of mixing between hybrid gabbros. However, the scatter in data for the main gabbros may be, at least in part, a result of local mixing between main gabbro and magmas from either, or both, of the hybrid gabbro groups.

Discussion/conclusions

The voluminous gabbroic rocks of the Fraser Zone are the mafic component of a regional sheeted sill complex (Spaggiari et al., 2011). Field relationships and recent geochronological data show that the gabbros intruded felsic country rock, including metasedimentary rocks deposited shortly prior to gabbro intrusion. They have also both intruded, and are intruded by, essentially comagmatic granitic magmas of the Recherche Supersuite (Spaggiari et al., 2011). Hybridization between mafic and felsic magmas is clearly developed, and several examples were sampled during the present study. Thus, within a very short period (almost within error of the SIMS (SHRIMP) dating), there occurred deposition of siliciclastic rocks in the Arid Basin, regional injection of voluminous gabbroic sheets, high-temperature metamorphism, and the generation of crustally derived felsic melts, in the form of both the regional Recherche Supersuite (which dominates the Nornalup Zone to the southeast) and more

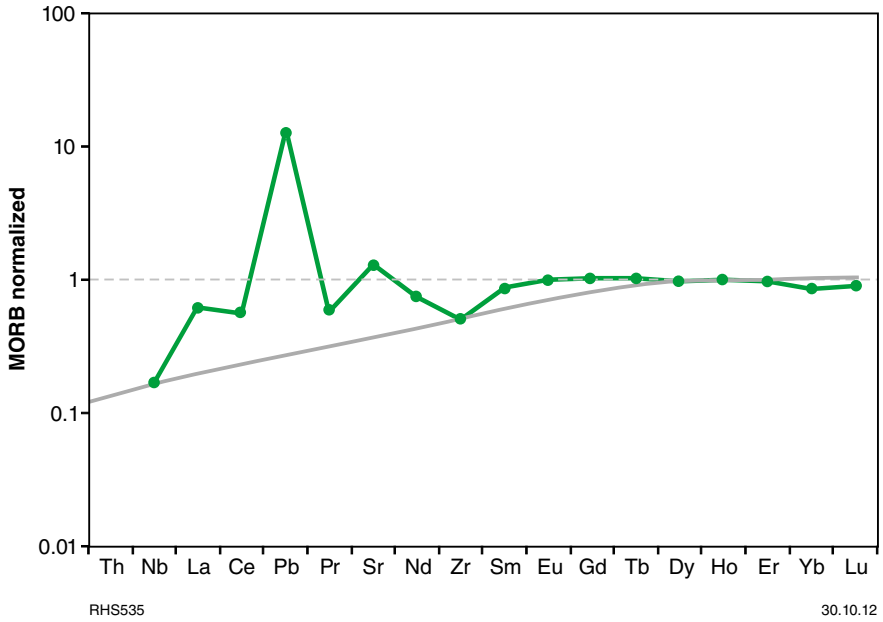

Figure 15. MORB-normalized incompatible trace element spidergram explaining the method employed to estimate the original composition of a mantle-melt parental to depleted gabbro sample GSWA 183624. The thick grey line defines the composition of the hypothetical parent to GSWA 183624 and gives the following concentrations (in ppm): Ba = 0.8, Th = 0.017, Nb = 0.4, La = 0.51, Ce = 1.9, Pb = 0.09, Pr = 0.46, Sr = 36, Nd = 3.3, Zr = 37, Sm = 1.6, Eu = 0.67, Gd = 2.5, Tb = 0.48, Dy = 3.5, Ho = 0.8, Er = 2.5, Yb = 2.65, Lu = 0.41. Normalizations after Sun and McDonough (1989).

locally developed, disequilibrium, anatectic melts of the siliciclastic country rocks.

Peak metamorphic pressures during this event reached 8–9 kbar (Oorschot, 2011), which could indicate the depth at which the presently exposed gabbros were intruded and also the minimum depth of the basin into which the siliciclastic rocks accumulated (25–30 km). However, this would assume no subsequent structural burial. Peak metamorphic temperature reached 800–850°C (Clark, 1999; Oorschot, 2011). It is unclear if these high temperatures were essentially the result of the intrusion of the gabbroic sheets or reflect an unsually high geotherm related to an underlying regional thermal anomaly. Similar P–T conditions (800–850°C and 5–7 kbar), estimated from c. 1300 Ma metasedimentary rocks of the Barren Basin (Coramup Gneiss) — located to the southwest in the Coramup Shear Zone in the southeastern Biranup Zone (Fig. 1; Bodorkos and Clark, 2004b) — also indicate the presence of a regional thermal anomaly during Stage I of the Albany–Fraser Orogeny. The tectonic setting of the Arid Basin is not known; however, basin formation, the regional thermal anomaly, formation of the gabbro sheet complex, high-temperature metamorphism, and regional granite magmatism are almost certainly directly linked.

Although Condie and Myers (1999) argued that the Fraser Zone represented the remnants of one or more oceanic arcs that were accreted at c. 1300 Ma during closure of a basin separating the West Australian (Yilgarn) and Mawson Cratons, this scenario now appears very unlikely. The isotopic data presented by Fletcher et al. (1991) alone suggest the gabbros cannot have formed in an oceanic arc environment simply because their bulk source involved too much old crust. Further, the geochemical arguments outlined in this Record indicate that simple assimilation of recognized basement components into a mantle derived melt is a more plausible explanation for the evolved compositions of the Fraser Zone gabbros than extraction from a subduction modified mantle. Our interpretations here do not rule out formation of the Fraser Zone gabbros in a subduction environment, but do severely question the basis on which previous authors have invoked that model. If there is any indication from the geochemistry of the gabbros for a subduction setting, it is from the requirement that the parental melts for at least some, and possibly all, of the gabbros were derived from a mantle source that was slightly more depleted, through prior melt extraction, than the source for modern MORB. If the Fraser Zone gabbros are subduction related, they do not represent an oceanic arc environment and there is no clear basis for linking the c. 1300 Ma event to any form of accretion.

Our preferred model for the petrogenesis of the Fraser Zone gabbros involves mantle upwelling beneath an intracontinental rift, backarc, or possibly continental arc. A continental arc seems least likely in view of the absence of calc-alkaline magmas in the Fraser Zone itself, although some components of the contemporaneous Recherche Supersuite in the adjacent Nornalup Zone have

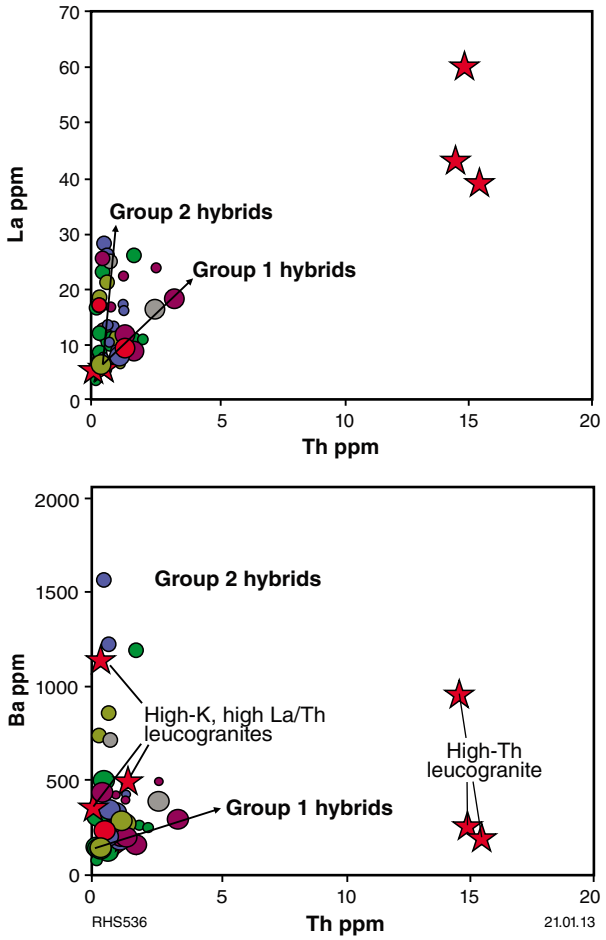

Figure 16. Compositional variation diagrams of variations in La and Ba against Th for unhybridized gabbros (main gabbros), both groups of hybrid gabbros, and granites that are interlayered with, and are comagmatic with, the gabbros. Symbols as for Figures 5 and 9. Large red stars denote high-Th granites.

calc-alkaline compositions. If the enriched trace element signatures in the high-Fe tholeiites that form the main gabbros are better explained by crustal contamination, then a distal back-arc or a truly intracontinental setting appears more likely than an arc-proximal setting.

In this model, mantle melt underplated and intraplated the base of the crust, where it assimilated a small (<10%) component of crust or melt derived from that crust. All of the geochemical modelling requires that the prior evolution of at least one of the components (mantle melt or crust) involved fractionation of garnet. The most likely candidate for the basement component is a combination of Archean granite and Munglinup Gneiss (or at least reworked Archean granite), both of which have high La/Yb ratios resulting from extraction from garnet-bearing sources. If this modelling is correct, it suggests that the Yilgarn Craton extended beneath the Fraser Zone.

Subsequent compositional evolution of the Fraser Zone gabbros was dominantly by closed system fractional crystallization (i.e. no further assimilation), until emplacement near or at the present level of exposure. At the same time, regional crustal anatexis generated leucosyenogranitic magmas that form the main felsic component of the Recherche Supersuite. These granites are interpreted to comprise a significant component of the Nornalup Zone (Myers, 1995; Nelson et al., 1995) and have also intruded the Fraser Zone. Geochronology and field evidence for intrusion contemporaneous with the Fraser Zone gabbros — including magma mingling textures — is consistent with geochemical evidence that Group 1 hybrid gabbros have incorporated small amounts of felsic magmas with typical Recherche Supersuite compositions. Rapid emplacement of the sheeted gabbro complex also resulted in extensive, low-degree, partial melting of the metasedimentary country rocks. The resulting high-K, disequilibrium, modal melts also mixed with the main gabbro magmas to form Group 2 hybrid gabbros. In addition, the scatter in data for the main gabbros may be, at least in part, a result of local further mixing between main gabbro and magmas from either, or both, hybrid groups.

This scenario resembles that predicted for the early stages in the development of a lower crustal hot-zone. According to this model, deep crustal hot zones formed through extensive mafic intraplating. A high intrusion rate can lead to a situation where each successive intrusion adds more heat to the lower crust than is conducted away. The model of Annen et al. (2006), predicts that within this emerging 'hot zone', ambient temperatures may eventually exceed the solidus temperature of both the mafic magma and of the country rock. Under such conditions, the country rock may partially melt, whereas the mafic sheets will retain a residual melt fraction (i.e. they will not fully crystallize). Mixing between the various partial and/or residual melts produces a range of magmatic compositions.

The hot zone model (Annen et al., 2006) was developed to explain the genesis of subduction-related felsic magmas in the lower crustal regions of a continental arc, but is equally applicable to a range of tectonic environments. In better developed cases, hot zones may evolve into regional-scale, compositionally homogenised, crystal mush chambers. This has clearly not happened within the exposed parts of the Fraser Zone, possibly because this zone reflects a higher crustal level, or thinner crust, than is the case in typical continental arc systems.

In view of recent Ni–Cu sulfide discoveries within rocks of the Fraser Zone (e.g. Nova, at The Eye prospect; Sirius Resources NL, 2012a,b), it is worth making a brief comment on the geochemistry of the main gabbros with respect to their potential to yield Ni–Cu mineralization, and on the Ni–Cu mineralization potential of the Fraser Zone in general. The main gabbros of the Fraser Zone have rather high Ni/Cu ratios (Ni/Cu = 2–3) and this also appears to be a feature of the Nova discovery (e.g. Sirius Resources NL, 2012a,b). In this respect it appears quite reasonable to relate the host gabbro at Nova to the main gabbro suite. If this is the case, then the entire Fraser Zone may be prospective for similar Ni–Cu sulfide

mineralization. Whereas the Ni concentration of the main gabbro is comparable to those of many other basalts globally with similar MgO contents, Cu concentrations are relatively low (average main gabbro ~54 ppm). This is also apparent in their low Cu/Zr ratios (typically <1). In view of the relatively unaltered nature of the rocks, it seems unlikely that Cu was mobile. Instead, Cu was likely extracted more efficiently than Ni as a result of either early sulfide segregation during magma crystallization, or retention of sulfide at the magma source. The hybridization processes leading to Group 1 and 2 hybrid gabbros are possibly not a cause of sulfur saturation in these magmas because the main gabbros (i.e. non-hybridized source) themselves are already depleted in Cu. If contamination by sulfur-rich country rock is a key to sulfur saturation in the main gabbros, then this process happened at a deeper level than that sampled here and involved different (deeper?) crustal components than those involved in production of the observed hybrid gabbros.

References

Adams, M 2012, Structural and geochronological evolution of the Malcolm Gneiss, Nornalup Zone, Albany–Fraser Orogen, Western Australia: Geological Survey of Western Australia, Record 2012/4, 132p.

Annen, C, Blundy, JD and Sparks, RSJ 2006, The genesis of intermediate and silicic magmas in deep crustal hot zones: Journal of Petrology, v. 47, p. 505–539.

Bodorkos, S and Clark, DJ 2004a, Evolution of a crustal-scale transpressive shear zone in the Albany Fraser Orogen, SW Australia: 2. Tectonic history of the Coramup Gneiss and a kinematic framework for Mesoproterozoic collision of the West Australian and Mawson cratons: Journal of Metamorphic Geology, v. 22, no. 8, p. 713–731, doi: 10.1111/j.1525-1314.2004.00544.x.

Bodorkos, S and Clark, DJ 2004b, Evolution of a crustal-scale transpressive shear zone in the Albany Fraser Orogen, SW Australia: 1. P–T conditions of Mesoproterozoic metamorphism in the Coramup Gneiss: Journal of Metamorphic Geology, v. 22, no. 8, p. 691–711, doi: 10.1111/j.1525-1314.2004.00543.x.

Cassidy, KF, Champion, DC, Krapež, B, Barley, ME, Brown, SJA, Blewett, RS, Groenewald, PB and Tyler, IM 2006, A revised geological framework for the Yilgarn Craton, Western Australia: Geological Survey of Western Australia, Record 2006/8, 8p.

Clark, DJ 1999, Thermo-tectonic evolution of the Albany–Fraser Orogen, Western Australia: University of New South Wales, Sydney, New South Wales, PhD thesis (unpublished).

Clark, DJ, Hensen, BJ and Kinny, PD 2000, Geochronological constraints for a two-stage history of the Albany–Fraser Orogen, Western Australia: Precambrian Research, v. 102, no. 3, p. 155–183.

Clark, DJ, Kinny, PD, Post, NJ and Hensen, BJ 1999, Relationships between magmatism, metamorphism and deformation in the Fraser Complex, Western Australia: constraints from new SHRIMP U–Pb zircon geochronology: Australian Journal of Earth Sciences, v. 46, p. 923–932.

Condie, KC and Myers, JS 1999, Mesoproterozoic Fraser Complex: geochemical evidence for multiple subduction-related sources of lower crustal rocks in the Albany–Fraser Orogen, Western Australia: Australian Journal of Earth Sciences, v. 46, p. 875–882.

Dawson, GC, Krapež, B, Fletcher, IR, McNaughton, N and Rasmussen, B 2003, 1.2 Ga thermal metamorphism in the Albany–Fraser Orogen of Western Australia: consequence of collision or regional heating by dyke swarms?: Journal of the Geological Society, London, v. 160, p. 29–37.

De Waele, B and Pisarevsky, SA 2008, Geochronology, paleomagnetism and magnetic fabric of metamorphic rocks in the northeast Fraser Belt, Western Australia: Australian Journal of Earth Sciences, v. 55, p. 605–621.

Doepel, JJG 1975, Albany–Fraser Province, in The geology of Western Australia: Geological Survey of Western Australia, Memoir 2, p. 94–102.

Fletcher, IR, Myers, JS and Ahmat, AL 1991, Isotopic evidence on the age and origin of the Fraser Complex, Western Australia: a sample of Mid-Proterozoic lower crust: Chemical Geology: Isotope Geoscience, v. 87, p. 197–216.

Geological Survey of Western Australia 2011, East Albany–Fraser and southeast Yilgarn, 2011 update: Geological Survey of Western Australia, Geological Exploration Package.

Gollam, M 2012, Final drilling report 'The Eye'; Sirius Gold Pty Ltd: Geological Survey of Western Australia, Statutory mineral exploration report, A092733 (unpublished).

Hall, CE, Jones, SA and Bodorkos, S 2008, Sedimentology, structure and SHRIMP zircon provenance of the Woodline Formation, Western Australia: implications for the tectonic setting of the West Australian Craton during the Paleoproterozoic: Precambrian Research, v. 162, p. 577–598, doi:10.1016/j.precamres.2007.11.001.

Jolly, WT, Lidiak, EG, Dickin, AP and Wu, T-U 2001, Secular geochemistry of central Puerto Rican island arc lavas: constraints on Mesozoic tectonism in the eastern Greater Antilles: Journal of Petrology, v. 42, p. 2197–2214.

Kirkland, CL, Spaggiari, CV, Pawley, MJ, Wingate, MTD, Smithies, RH, Howard, HM, Tyler, IM, Belousova, EA and Poujol, M 2011a, On the edge: U–Pb, Lu–Hf, and Sm–Nd data suggests reworking of the Yilgarn Craton margin during formation of the Albany–Fraser Orogen: Precambrian Research, v. 187, p. 223–247, doi:10.1016/j.precamres.2011.03.002.

Kirkland, CL, Spaggiari, CV, Wingate, MTD, Smithies, RH, Belousova, EA, Murphy, R and Pawley, MJ 2011b, Inferences on crust–mantle interaction from Lu–Hf isotopes: a case study from the Albany–Fraser Orogen: Geological Survey of Western Australia, Record 2011/12, 25p.

Kirkland, CL, Wingate, MTD and Spaggiari, CV 2011c, 194714: psammitic gneiss, Gnamma Hill; Geochronology Record 999: Geological Survey of Western Australia, 6p.

Kirkland, CL, Wingate, MTD and Spaggiari, CV 2011d, 194718: mafic granulite, American Granulite Quarry; Geochronology Record 993: Geological Survey of Western Australia, 4p.

Kirkland, CL, Wingate, MTD and Spaggiari, CV 2011e, 194715: leucosome in psammitic gneiss, Gnamma Hill; Geochronology Record 1000: Geological Survey of Western Australia, 4p.

Kirkland, CL, Wingate, MTD and Spaggiari, CV 2012, 194711, metamonzogranite, Kent Dam; Geochronology Record 1044: Geological Survey of Western Australia, 4p.

Myers, JS 1985, The Fraser Complex: a major layered intrusion in Western Australia, *in* Professional papers for 1983: Geological Survey of Western Australia, Report 14, p. 57–66.

Myers, JS 1990, Albany–Fraser Orogen, in Geology and mineral resources of Western Australia: Geological Survey of Western Australia, Memoir 3, p. 255–263.

Myers, JS 1995, Geology of the Esperance 1:1 000 000 sheet (2nd edition): Geological Survey of Western Australia, 1:1 000 000 Geological Series Explanatory Notes, 10p.

Myers, JS, Shaw, RD and Tyler, IM 1996, Tectonic evolution of Proterozoic Australia: Tectonics, v. 15, p. 1431–1146.

Nelson, DR 1995, 83691: biotite monzogranite gneiss, north of Young River; Geochronology Record 79: Geological Survey of Western Australia, 4p.

Nelson, DR, Myers, JS and Nutman, AP 1995, Chronology and evolution of the Middle Proterozoic Albany–Fraser Orogen, Western Australia: Australian Journal of Earth Sciences, v. 42, p. 481–495.

Oorschot, CW 2011, P–T–t evolution of the Fraser Zone, Albany–Fraser Orogen, Western Australia: Geological Survey of Western Australia, Record 2011/18, 101p.

Pawley, MJ, Wingate, MTD, Kirkland, CL, Wyche, S, Hall, CE, Romano, SS and Doublier, MP 2012, Adding pieces to the puzzle: episodic crustal growth and a new terrane in the northeast Yilgarn Craton, Western Australia: Australian Journal of Earth Sciences, v. 59, no. 5, p. 603–623.

Rasmussen, B, Fletcher, IR, Bengtson, S and McNaughton, N 2004, SHRIMP U–Pb dating of diagenetic xenotime in the Stirling Range Formation, Western Australia: 1.8 billion year minimum age for the Stirling biota: Precambrian Research, v. 133, p. 329–337.

Sinton, JM, Ford, LL, Chappell, B and McCulloch, MT 2003, Magma genesis and mantle heterogeneity in the Manus back-arc basin, Papua New Guinea: Journal of Petrology, v. 44, p. 159–195.

Sirius Resources NL 2012a, Best hit yet at Nova: Report to Australian Securities Exchange, 26 September 2012, 5p.

Sirius Resources NL 2012b, First diamond hole intersects sulphide where expected at Nova: Report to Australian Securities Exchange, 20 August 2012, 5p.

Spaggiari, CV, Bodorkos, S, Barquero-Molina, M, Tyler, IM and Wingate, MTD 2009, Interpreted bedrock geology of the south Yilgarn and central Albany–Fraser Orogen, Western Australia: Geological Survey of Western Australia, Record 2009/10, 84p.

Spaggiari, CV, Kirkland, CL, Pawley, MJ, Smithies, RH, Wingate, MTD, Doyle, MG, Blenkinsop, TG, Clark, C, Oorschot, CW, Fox, LJ and Savage, J 2011, The Geology of the east Albany–Fraser Orogen — a field guide: Geological Survey of Western Australia, Record 2011/23, 97p.

Spaggiari, CV, Kirkland, CL, Smithies, RH and Wingate, MTD 2012, What lies beneath — interpreting the Eucla basement, *in* GSWA 2012 extended abstracts: promoting the prospectivity of Western Australia: Geological Survey of Western Australia, Record 2012/2, p. 25–27.

Spaggiari, CV and Pawley, MJ 2012a, Interpreted pre-Mesozoic bedrock geology of the Tropicana region of the east Albany–Fraser Orogen (1:250 000), *in* The geology of the east Albany–Fraser Orogen — a field guide *compiled by* CV Spaggiari, CL Kirkland, MJ Pawley, RH Smithies, MTD Wingate, MG Doyle, TG Blenkinsop, C Clark, CW Oorschot, LJ Fox, and J Savage: Geological Survey of Western Australia, Record 2011/23, Plate 2.

Spaggiari, CV and Pawley, MJ 2012b, Interpreted pre-Mesozoic bedrock geology of the east Albany–Fraser Orogen and southeast Yilgarn Craton (1:500 000), *in* The geology of the east Albany–Fraser Orogen — a field guide *compiled by* CV Spaggiari, CL Kirkland, MJ Pawley, RH Smithies, MTD Wingate, MG Doyle, TG Blenkinsop, C Clark, CW Oorschot, LJ Fox, and J Savage: Geological Survey of Western Australia, Record 2011/23, Plate 1.

Spaggiari, CV and Pawley, MJ 2012c, Interpreted pre-Mesozoic bedrock geology of the east Albany–Fraser Orogen and southeast Yilgarn Craton (1:500 000), *in* The geology of the east Albany–Fraser Orogen — a field guide *compiled by* CV Spaggiari, CL Kirkland, MJ Pawley, RH Smithies, MTD Wingate, MG Doyle, TG Blenkinsop, C Clark, CW Oorschot, LJ Fox, and J Savage: Geological Survey of Western Australia, Record 2011/23, Plate 1A.

Sun, S-S and McDonough, WF 1989, Chemical and isotopic systematics of oceanic basalts: implications for mantle compositions and processes, *in* Magmatism in the Ocean Basins *edited by* AD Saunders and MJ Norry: Geological Society, London, Special Publication 42, p. 313–345.

Vallini, DA, Rasmussen, B, Krapež, B, Fletcher, IR and McNaughton, N 2005, Microtextures, geochemistry and geochronology of authigenic xenotime constraining the cementation history of a Paleoproterozoic metasedimentary sequence: Sedimentology, v. 52, p. 101–122.

Wingate, MTD and Bodorkos, S 2007, 177910: metamorphosed quartz sandstone, Peters Dam; Geochronology Record 660: Geological Survey of Western Australia, 6p.

Appendix 1

List of GSWA geochemistry samples used in this Record

GSWA Sample	Magmatic series	WAROX siteno	WAROX siteid	Easting	Northing	100k map	250k map	Location
183665	Main gabbro	542206	HMHEAF000021	502081	6447100	3533	SI 51-3	14 km west of Newman Rock
183663	Main gabbro	542205	HMHEAF000020	502587	6447060	3533	SI 51-3	14 km west of Newman Rock
183654	Main gabbro	542196	HMHEAF000011	486972	6433755	3433	SI 51-2	Mt Malcolm
183652	Main gabbro	542195	HMHEAF000010	486546	6433715	3433	SI 51-2	Mt Malcolm
183651	Main gabbro	542194	HMHEAF000009	486500	6433831	3433	SI 51-2	Mt Malcolm
183649	Main gabbro	542193	HMHEAF000008	486499	6434005	3433	SI 51-2	Mt Malcolm
183647	Main gabbro	542192	HMHEAF000007	486382	6434394	3433	SI 51-2	Mt Malcolm
183623	Main gabbro	544426	CVSEAF000185	477635	6432372	3433	SI 51-2	Near Gnamma Hill
183668	Main gabbro	553693	CVSEAF000217	510397	6453922	3533	SI 51-3	Quarry NW of Newman Rocks
183632	Main gabbro	544432	CVSEAF000191	485325	6434615	3433	SI 51-2	Southeast of Verde Austral Quarry
183635	Main gabbro	551356	CVSEAF000193	485426	6434584	3433	SI 51-2	Southeast of Verde Austral Quarry
183639	Main gabbro	551360	CVSEAF000197	485565	6434543	3433	SI 51-2	Southeast of Verde Austral Quarry
183629	Main gabbro	544429	CVSEAF000188	485398	6435250	3433	SI 51-2	Southeast of Verde Austral Quarry
183633	Main gabbro	544433	CVSEAF000192	485385	6434584	3433	SI 51-2	Southeast of Verde Austral Quarry
183640	Main gabbro	551362	CVSEAF000199	485861	6434539	3433	SI 51-2	Southeast of Verde Austral Quarry
183641	Main gabbro	551363	CVSEAF000200	486030	6434574	3433	SI 51-2	Southeast of Verde Austral Quarry
183670	Main gabbro	553711	CVSEAF000219	508491	6460310	3534	SH 51-15	Track north of Eyre Highway
183669	Main gabbro	553710	CVSEAF000218	507442	6462074	3534	SH 51-15	Track north of Eyre Highway
183655	Main gabbro	542197	HMHEAF000012	480236	6455358	3433	SI 51-2	Wyralinu Hill, Fraser Range
183656	Main gabbro	542198	HMHEAF000013	480298	6455294	3433	SI 51-2	Wyralinu Hill, Fraser Range
183659	Main gabbro	542201	HMHEAF000016	480590	6454996	3433	SI 51-2	Wyralinu Hill, Fraser Range
183657	Main gabbro	542199	HMHEAF000014	480377	6455190	3433	SI 51-2	Wyralinu Hill, Fraser Range
183643	Group 1 hybrid	542188	HMHEAF000003	486215	6434505	3433	SI 51-2	Mt Malcolm
183630	Group 1 hybrid	544430	CVSEAF000189	485025	6434869	3433	SI 51-2	Southeast of Verde Austral Quarry
183675	Group 1 hybrid	553712	CVSEAF000220	507068	6464149	3534	SH 51-15	Track north of Eyre Highway
183673	Group 1 hybrid	553715	CVSEAF000223	507255	6464152	3534	SH 51-15	Track north of Eyre Highway
183626	Group 1 hybrid	504782	CVSEAF000026	484947	6435488	3433	SI 51-2	Verde Austral Quarry
183661	Group 1 hybrid	542203	HMHEAF000018	482290	6456317	3433	SI 51-2	Wyralinu Hill, Fraser Range
183662	Group 1 hybrid	542204	HMHEAF000019	482290	6456242	3433	SI 51-2	Wyralinu Hill, Fraser Range
183660	Group 1 hybrid	542202	HMHEAF000017	482222	6456500	3433	SI 51-2	Wyralinu Hill, Fraser Range
183664	Group 2 hybrid	542206	HMHEAF000021	502081	6447100	3533	SI 51-3	14 km west of Newman Rock

Appendix 1 (continued)

GSWA Sample	Magmatic series	WAROX siteno	WAROX siteid	Easting	Northing	100k map	250k map	Location
183648	Group 2 hybrid	553735	HMHEAF000022	486477	6434054	3433	SI 51-2	Mt Malcolm
183646	Group 2 hybrid	542191	HMHEAF000006	486342	6434466	3433	SI 51-2	Mt Malcolm
183645	Group 2 hybrid	542190	HMHEAF000005	486253	6434398	3433	SI 51-2	Mt Malcolm
183644	Group 2 hybrid	542189	HMHEAF000004	486230	6434450	2233	SI 51-2	Mt Malcolm
183636	Group 2 hybrid	551357	CVSEAF000194	485471	6434577	3433	SI 51-2	Southeast of Verde Austral Quarry
183634	Group 2 hybrid	544433	CVSEAF000192	485385	6434584	3433	SI 51-2	Southeast of Verde Austral Quarry
183622	Group 2 hybrid	544421	CVSEAF000180	475248	6442599	3433	SI 51-2	Track into Southern Hills station
183674	Group 2 hybrid	553716	CVSEAF000224	507148	6464172	3534	SH 51-15	Track north of Eyre Highway
183672	Group 2 hybrid	553714	CVSEAF000222	507241	6464154	3534	SH 51-15	Track north of Eyre Highway
183627	Group 2 hybrid	504782	CVSEAF000026	484947	6435488	3433	SI 51-2	Verde Austral Quarry
183658	Group 2 hybrid	542200	HMHEAF000015	480456	6455098	3433	SI 51-2	Wyralinu Hill, Fraser Range
177909	High-Th leucogranite	255753	DRN177909	491173	6465549	3434	SH 51-14	Fantasia Quarry
194711	High-Th leucogranite	504777	CVSEAF000021	492904	6418535	3433	SI 51-2	Newman Shear Zone
194719	High-Th leucogranite	504787	CVSEAF000031	503090	6475794	3534	SH 51-15	Symons Hill
183642	High-K, La/Th leucogranite	542187	HMHEAF000002	486177	6434525	3433	SI 51-2	Mt Malcolm
183625	High-K, La/Th leucogranite	544428	CVSEAF000187	484560	6437593	3433	SI 51-2	North of Verde Austral Quarry
183631	High-K, La/Th leucogranite	544431	CVSEAF000190	484928	6435002	3433	SI 51-2	Southeast of Verde Austral Quarry
183628	High-K, La/Th leucogranite	504782	CVSEAF000026	484947	6435488	3433	SI 51-2	Verde Austral Quarry

Appendix 2

Geochemical analyses

		Major elements (wt%)												
	Sample No.	SiO_2	TiO_2	Al_2O_3	Fe_2O_3T	MgO	MnO	CaO	K_2O	Na_2O	P_2O_5	LOI	SO_3	Mg#
Main gabbro	183622	48.91		15.96	10.89	7.94	0.22	9.88	0.81	2.08	0.16	1.65	0.23	59
	183623	48.41	1.07	16.98	10.82	8.95	0.17	9.88	0.58	2.29	0.16	0.49	0.06	62
	183624	47.28	1.01	17.53	12.45	8.79	0.19	10.40	0.17	1.59	0.06	0.28	0.17	58
	183629	46.66	0.83	15.96	10.85	11.90	0.17	9.10	0.51	2.17	0.13	1.22	0.29	68
	183632	47.47	0.93	15.29	11.43	11.42	0.18	10.00	0.41	1.85	0.13	0.66	0.06	66
	183633	48.77	1.21	15.77	12.31	7.27	0.20	9.59	0.76	2.25	0.22	1.49	0.04	54
	183635	46.78	1.12	16.86	10.87	9.69	0.17	9.66	0.53	2.12	0.20	1.54	0.28	64
	183637	49.12	1.43	15.35	12.17	7.32	0.21	9.53	0.59	2.38	0.28	1.46	0.02	54
	183638	49.91	1.16	15.10	11.54	7.70	0.23	10.92	0.42	2.26	0.18	0.44	0.03	57
	183639	46.73	1.16	15.99	11.59	10.43	0.18	8.96	0.58	2.38	0.20	1.41	0.23	64
	183640	49.78	1.29	15.92	11.23	7.92	0.19	9.06	0.89	2.48	0.21	0.86	0.03	58
	183641	47.22	1.25	16.08	11.18	8.93	0.18	10.10	0.47	2.30	0.18	1.75	0.25	61
	183647	49.11	0.98	16.46	10.54	8.44	0.18	10.27	0.76	2.08	0.14	0.89	0.04	61
	183649	48.46	1.41	15.99	11.82	8.03	0.19	10.00	0.65	2.45	0.18	0.67	0.03	57
	183651	45.75	0.96	17.03	10.37	11.65	0.16	9.44	0.31	2.17	0.13	1.74	0.18	69
	183654	46.10	1.05	17.55	11.24	9.62	0.17	9.98	0.23	2.16	0.09	1.47	0.23	63
	183655	49.87	1.50	14.78	12.49	6.89	0.25	10.23	0.68	2.52	0.25	0.13	0.29	52
	183656	48.02	1.68	15.54	12.61	7.15	0.28	9.95	0.77	2.17	0.42	1.00	0.27	53
	183657	48.29	1.69	15.84	12.54	7.46	0.22	9.28	1.00	2.30	0.33	0.61	0.27	54
	183659	48.95	1.58	16.13	12.73	6.93	0.25	9.47	1.03	2.21	0.31	0.02	0.25	52
	183663	47.59	1.01	17.53	10.65	8.75	0.17	9.91	0.57	2.39	0.17	0.89	0.25	62
	183665	47.85	1.22	17.27	11.84	8.21	0.19	9.95	0.39	2.63	0.11	-0.02	0.26	58
	183668	47.02	0.68	16.31	10.39	13.12	0.16	10.13	0.27	1.83	0.11	-0.39	0.23	71
	183670	47.78	0.94	17.00	10.68	9.78	0.17	10.56	0.34	2.20	0.14	0.00	0.27	64
Group 1 hybrid	183626	50.21	1.28	14.73	11.83	7.07	0.20	9.78	0.94	2.83	0.19	0.51	0.28	54
	183630	47.09	0.94	15.66	11.63	11.40	0.22	9.43	0.48	1.82	0.18	0.79	0.20	66
	183643	47.63	0.92	16.97	10.57	10.10	0.17	9.74	0.55	2.10	0.16	0.69	0.25	65
	183660	47.46	1.33	15.56	11.94	7.31	0.22	9.03	1.00	2.29	0.22	3.45	0.06	55
	183661	47.55	1.34	16.40	12.96	8.20	0.23	9.59	0.53	2.25	0.20	0.62	0.02	56
	183662	49.60	1.09	16.19	11.58	7.88	0.21	9.03	0.59	2.30	0.13	1.19	0.09	57
	183673	49.36	1.25	15.68	12.27	8.14	0.20	10.51	0.48	2.32	0.22	-0.86	0.31	57
	183675	46.94	0.86	16.44	11.08	11.50	0.18	10.32	0.28	1.96	0.16	-0.13	0.24	67
Group 2 hybrid	183627	48.85	2.18	13.25	16.08	4.77	0.26	8.74	1.06	2.86	0.36	1.07	0.38	37
	183634	56.52	1.07	15.29	10.11	3.97	0.21	6.94	1.83	2.97	0.24	0.63	0.01	44
	183636	55.23	1.87	15.07	12.44	2.50	0.25	6.27	2.09	2.80	0.43	0.81	0.01	28
	183644	51.89	1.49	19.49	9.54	2.90	0.19	7.20	1.03	3.98	0.33	1.79	0.01	38
	183645	50.54	1.03	16.10	10.02	7.83	0.18	10.65	0.46	2.43	0.12	0.54	0.03	61
	183646	49.76	1.22	15.54	10.82	7.31	0.19	9.76	0.79	2.51	0.15	1.79	0.02	57
	183648	55.48	1.06	15.62	8.50	4.88	0.15	8.40	0.80	2.93	0.15	1.90	0.02	53
	183658	51.46	1.46	15.88	10.99	4.87	0.23	8.60	1.37	2.85	0.27	1.88	0.02	47
	183672	51.99	1.40	15.29	12.10	5.07	0.21	8.73	1.29	2.68	0.23	0.86	0.01	45
	183674	58.02	0.94	14.50	9.18	4.18	0.18	6.77	1.65	2.72	0.18	1.50	0.02	47

Appendix 2 (continued)

	Trace elements (ppm)															
	Sample No.	Cr	Ni	V	Sc	Cu	Zn	Ba	Sr	Rb	Cs	Pb	U	Th	Zr	Hf	Y
Main gabbro	183622	288	129	187	28	46	78	275	177.3	35.8	0.91	7	0.17	0.52	93	2.58	21.9
	183623	280	207	189	31	57	82	312	173.4	15.0	0.68	7	0.32	0.98	102	2.64	22.7
	183624	140	157	214	36	58	93	85	118.0	1.1	-0.03	4	-0.01	-0.05	37	1.29	26.6
	183629	683	472	132	24	120	78	222	164.5	13.9	0.67	6	0.34	1.06	88	2.3	20.3
	183632	442	332	209	34	60	83	202	123.1	8.9	0.36	6	0.18	0.61	86	1.97	23.2
	183633	190	132	181	27	51	97	476	172.0	21.0	0.59	10	0.43	1.26	128	4	31.2
	183635	280	342	160	26	57	85	350	211.8	10.9	0.44	7	0.26	0.68	159	3.72	23.2
	183637	334	94	192	31	61	100	450	195.8	6.1	-0.03	9	0.04	-0.05	89	2.99	22.4
	183638	233	79	217	34	39	85	270	204.6	2.3	-0.03	6	-0.01	-0.05	83	2.26	23.3
	183639	328	280	165	25	42	89	329	228.8	12.6	0.44	7	0.3	0.92	144	3.39	24.8
	183640	252	173	193	26	63	89	421	203.3	23.3	0.56	10	0.43	1.32	169	4.47	30.8
	183641	216	176	195	30	47	83	239	184.7	9.9	0.34	7	0.21	0.74	109	2.77	27.8
	183647	220	137	192	29	53	75	253	244.3	24.2	1.11	6	0.54	2.14	82	2.39	22.8
	183649	253	131	230	33	62	90	264	219.2	18.4	0.81	7	0.41	1.77	129	3.23	34.1
	183651	157	351	146	21	33	72	139	233.0	5.7	0.18	4	0.1	0.25	77	1.91	18.1
	183654	79	196	193	30	46	78	76	221.1	3.9	0.14	4	0.04	0.18	72	1.91	21.1
	183655	171	76	221	34	52	95	242	170.3	7.6	0.04	9	0.21	0.81	117	3.51	37.5
	183656	276	101	210	30	41	105	424	262.0	22.5	0.31	9	0.22	0.95	148	3.45	34.7
	183657	228	125	196	26	40	99	496	232.6	31.8	1.16	11	0.63	2.62	156	3.88	34.4
	183659	164	117	174	28	36	106	402	198.7	38.6	0.68	11	0.3	1.28	150	4.22	34.5
	183663	216	202	141	24	61	76	269	217.7	13.5	0.51	6	0.33	0.82	92	2.68	22.3
	183665	83	120	217	33	49	79	120	218.8	8.9	0.45	4	0.16	0.65	85	2.28	24.7
	183668	346	367	144	24	69	70	146	135.5	7.1	0.25	5	0.17	0.52	63	1.59	16.2
	183670	316	229	179	27	58	77	191	195.8	7.1	0.22	5	0.19	0.74	69	1.8	21.3
Group 1 hybrid	183626	284	86	227	34	47	93	384	136.4	30.3	1.45	10	0.77	2.59	133	3.53	33.6
	183630	452	357	172	28	64	82	182	210.6	13.5	0.59	5	0.27	1.15	72	1.67	19
	183643	327	280	146	25	61	79	244	176.4	15.6	0.74	7	0.36	1.17	105	2.26	21.5
	183660	221	134	165	24	33	93	287	194.6	40.6	2.04	10	0.73	3.39	97	3.05	28.7
	183661	241	134	187	31	42	99	193	184.8	16.4	0.64	7	0.33	1.4	103	2.52	28.2
	183662	311	97	188	31	46	89	155	167.7	21.7	1.58	6	0.44	1.76	77	2.08	23.9
	183673	249	92	217	32	54	91	283	191.1	11.9	0.4	6	0.31	1.18	86	2	28.3
	183675	413	287	187	27	41	76	140	219.4	5.7	0.15	4	0.17	0.42	58	1.42	15.4
Group 2 hybrid	183627	34	26	324	38	52	137	720	155.1	18.9	0.21	12	0.28	0.73	239	6.19	55.8
	183634	86	57	127	24	33	94	1229	210.4	32.2	0.37	15	0.26	0.66	202	5.82	33.9
	183636	26	16	170	28	27	126	1564	243.3	35.1	0.31	16	0.33	0.49	337	8.87	39.1
	183644	56	37	123	17	38	87	503	331.9	8.2	0.13	12	0.31	0.47	447	11.8	18
	183645	107	117	200	31	68	71	139	221.3	4.2	0.08	6	0.1	0.35	71	2.01	22
	183646	267	119	213	30	50	81	329	217.4	20.8	0.33	8	0.16	0.33	101	3	27
	183648	144	74	147	23	42	68	312	225.1	6.9	0.1	10	0.1	0.24	90	2.68	25.4
	183658	117	46	176	26	38	90	442	190.8	33.7	0.13	14	0.2	0.45	125	3.84	35.6
	183672	114	41	224	32	38	106	737	207.4	18.9	0.12	11	0.17	0.31	172	4.14	32.6
	183674	131	60	133	23	33	86	856	208.7	25.1	0.23	12	0.3	0.66	174	4.82	30.7

Appendix 2 (continued)

		Trace elements (ppm)														
	Sample No.	Nb	Ta	La	Ce	Pr	Nd	Sm	Eu	Gd	Tb	Dy	Ho	Er	Yb	Lu
Main gabbro	183622	4.1	0.23	12.27	27.99	3.28	15.33	3.75	1.07	4.50	0.65	4.20	0.90	2.55	2.26	0.28
	183623	3.8	0.18	11.01	24.78	3.11	14.78	3.71	1.32	4.65	0.69	4.34	0.96	2.73	2.36	0.31
	183624	0.4	-0.05	1.56	4.25	0.77	5.45	2.29	1.02	3.75	0.69	4.42	1.02	2.90	2.65	0.41
	183629	3.3	0.15	8.94	20.7	2.5	12.14	2.97	1.02	3.71	0.52	3.52	0.77	2.13	1.97	0.25
	183632	2.9	0.11	8.06	18.51	2.34	11.48	2.80	1.05	3.93	0.59	3.96	0.91	2.62	2.38	0.33
	183633	7	0.36	17.63	39.34	4.7	22	4.86	1.58	6.07	0.88	5.53	1.25	3.41	3.10	0.44
	183635	5.2	0.26	13.64	31.37	3.92	18.99	4.45	1.55	5.04	0.73	4.50	0.97	2.73	2.40	0.34
	183637	7.7	0.45	16.53	38.48	4.8	24.02	6.13	2.01	7.31	1.05	6.52	1.43	3.86	3.12	0.41
	183638	4.3	0.22	10.02	23.13	2.94	14.72	3.89	1.29	4.67	0.68	4.23	0.97	2.77	2.39	0.32
	183639	4.7	0.23	13.34	30.75	3.76	18.22	4.35	1.47	5.12	0.73	4.50	0.98	2.78	2.44	0.34
	183640	5.7	0.31	16.25	36.59	4.51	20.52	5.05	1.46	5.70	0.84	5.27	1.13	3.21	2.83	0.41
	183641	4.1	0.2	10.58	24.72	3.25	15.88	3.99	1.39	5.26	0.76	4.95	1.10	3.10	2.66	0.35
	183647	3.3	0.17	11.4	25.58	3.2	14.83	3.55	1.11	3.85	0.60	3.76	0.83	2.25	1.94	0.25
	183649	4.3	0.22	11.88	28.45	3.72	18.17	4.57	1.50	5.17	0.81	4.95	1.08	2.88	2.63	0.38
	183651	2.4	0.1	6.42	15.81	2.11	11.17	3.01	1.05	3.41	0.53	3.34	0.74	1.98	1.77	0.21
	183654	1.3	-0.05	3.6	9.89	1.47	8.81	2.74	1.10	3.45	0.56	3.69	0.78	2.12	1.93	0.29
	183655	6.8	0.37	16.9	39.1	4.77	22.63	5.47	1.60	6.29	1.00	5.89	1.32	3.57	3.23	0.44
	183656	12.1	0.64	25.27	56.44	6.56	30.04	6.24	1.81	6.55	0.99	5.68	1.23	3.27	2.86	0.41
	183657	9.6	0.53	23.88	51.38	6.14	27.96	5.67	1.84	6.25	0.95	5.65	1.24	3.32	2.84	0.42
	183659	8.6	0.49	22.34	49.46	5.81	26.29	5.73	1.75	6.35	1.00	5.88	1.27	3.43	3.09	0.43
	183663	3.9	0.18	10.5	24.23	3.07	15.59	3.77	1.31	4.34	0.65	4.31	0.93	2.51	2.28	0.30
	183665	1.6	0.07	5.38	13.74	1.94	10.55	3.29	1.19	4.12	0.65	4.24	0.92	2.50	2.21	0.32
	183668	2.3	0.12	6.57	14.75	1.97	8.95	2.39	0.80	2.72	0.46	3.12	0.60	1.72	1.67	0.24
	183670	2.4	0.12	7.46	17.24	2.33	10.79	3.16	1.07	3.42	0.56	3.57	0.74	2.13	2.03	0.31
Group 1 hybrid	183626	5.4	0.3	16.38	36.93	4.52	21.32	5.10	1.56	6.37	0.93	5.85	1.36	3.87	3.38	0.48
	183630	3.2	0.15	8.8	20.68	2.5	12.2	2.81	0.98	3.57	0.48	3.28	0.72	2.05	1.90	0.23
	183643	3.9	0.2	10.54	23.99	2.96	14.22	3.37	1.20	3.99	0.61	3.74	0.83	2.30	1.98	0.28
	183660	7.2	0.43	18.26	40.11	4.62	20.72	4.77	1.41	5.13	0.82	4.86	1.06	2.92	2.55	0.35
	183661	4.9	0.27	11.8	27.55	3.39	16.49	4.07	1.35	4.86	0.79	4.83	1.09	2.87	2.58	0.36
	183662	2.9	0.16	8.86	20.14	2.49	12.69	3.35	1.18	4.17	0.68	4.27	0.95	2.68	2.35	0.34
	183673	3.4	0.19	11.32	25.5	3.45	15.58	4.24	1.34	4.74	0.80	5.05	1.04	2.91	2.78	0.42
	183675	2.1	0.12	6.33	14.38	1.92	9.25	2.58	0.92	2.76	0.43	2.99	0.60	1.63	1.68	0.22
Group 2 hybrid	183627	10.2	0.59	24.95	56.95	7.17	34.1	8.60	2.50	10.32	1.55	9.60	2.18	6.11	5.37	0.79
	183634	11	0.6	26.08	54.25	6.52	28.98	6.68	2.27	7.35	0.99	6.33	1.35	3.98	3.55	0.50
	183636	17.9	1.06	28.25	60.47	7.34	35.14	8.27	3.15	9.02	1.24	7.54	1.64	4.60	4.08	0.59
	183644	12.3	0.61	23.32	44.87	4.98	21.9	3.99	2.44	4.10	0.54	3.19	0.68	1.84	1.82	0.25
	183645	2.8	0.15	8.65	20.42	2.6	13.15	3.38	1.18	3.92	0.62	3.88	0.86	2.30	2.05	0.28
	183646	4.1	0.22	12.27	28.32	3.59	17.34	4.25	1.39	4.86	0.75	4.75	1.04	2.78	2.57	0.35
	183648	4.2	0.22	16.73	34.31	4.04	18.32	4.31	1.71	4.64	0.74	4.29	0.94	2.48	2.18	0.31
	183658	10.3	0.67	25.57	56.11	6.61	29.73	6.66	1.68	7.02	1.07	6.53	1.42	3.72	3.32	0.45
	183672	7.6	0.41	18.48	41.08	5.38	23.41	6.03	1.82	6.13	0.97	6.10	1.20	3.53	3.26	0.45
	183674	8.6	0.45	21.4	43.23	5.51	23.84	6.07	1.84	5.55	0.87	5.42	1.12	3.04	3.00	0.44

Appendix 3

Petrographic summaries of main rock types

All of the gabbros studied here show a high-grade metamorphic mineralogical and/or textural overprint. The main gabbros range in texture from near pristine intergranular to subophitic igneous textures, to granoblastic textures, and this full range can be observed at any one locality. A foliation is typically well-developed in zones of higher strain but in many cases is overprinted by a granoblastic texture. Even samples that show well-preserved subophitic textures typically include domains where primary pyroxene has been recrystallised to a granoblastic mass of metamorphic pyroxene or brown hornblende.

The main gabbros are generally fine- to medium-grained, mesocratic olivine gabbro to olivine gabbronorite. Plagioclase ranges in composition between An_{55} and An_{70} and forms 35–60% of the rock. Olivine forms up to 15% of the rock, mainly as anhedral to subhedral crystals partially enclosed within orthopyroxene. Pyroxene is typically intergranular, poikilitic, or granoblastic, and the abundance of clinopyroxene generally exceeds that of orthopyroxene. Magnetite forms anhedral crystals, constitutes up to 5% of the mode, and is commonly rimmed by brown biotite. Biotite itself can constitute up to 10% of some rocks. In many rocks with well-preserved igneous textures, biotite rims magnetite and is, in turn, rimmed by brown hornblende. In granoblastic rocks, biotite is either absent or forms flakes, which are in some cases strongly aligned with the general foliation. Brown hornblende is a notable component of most of the rocks, forming up to 20% of the mode. It rims biotite and pyroxene, commonly as granoblastic aggregates.

Group 1 hybrid gabbros are fine- to medium-grained, mesocratic rocks which, in some cases, preserve an igneous intergranular to subophitic texture but more commonly show a well-developed granoblastic texture. They differ from the main gabbros in that they typically contain less, or no, olivine and some samples contain rare interstitial quartz. Some samples from Wyralinu Hill also contain garnet poikioblasts up to 6 mm in size. Although hornblende is typically brown, it can range to brown-green to green.

Group 2 hybrid gabbros form two broad end-member textural types. The first, and possibly less common, type shows textural and mineralogical similarities to granoblastic-textured Group 1 hybrid gabbros but contains no olivine. The second type is typically fine to medium grained and texturally very inhomogeneous. It comprises fine-grained granoblastic domains similar to the first type of Group 2 hybrid gabbros. These enclose felsic domains forming bands, elongate blebs, or wisps, up to 3 cm long. The felsic domains typically contain no mafic minerals but comprise a medium- to coarse-grained granoblastic assemblage of plagioclase (commonly antiperthitic), lesser amounts of quartz, and vary rare perthite.

RECORD 2013/5

PETROGENESIS OF GABBROS OF THE MESOPROTEROZOIC FRASER ZONE: CONSTRAINTS ON THE TECTONIC EVOLUTION OF THE ALBANY–FRASER OROGEN

Smithies et al.

This Record is published in digital format (PDF) and is available as a free download from the DMP website at <http://www.dmp.wa.gov.au/GSWApublications>.

Further details of geological products produced by the Geological Survey of Western Australia can be obtained by contacting:

Information Centre
Department of Mines and Petroleum
100 Plain Street
EAST PERTH WESTERN AUSTRALIA 6004
Phone: (08) 9222 3459 Fax: (08) 9222 3444
http://www.dmp.wa.gov.au/GSWApublications